THE UNIVERSITY of EDINBURGH

Edinburgh Research Explorer

An experimental and numerical study on the effects of leakages and ventilation conditions on informal settlement fire dynamics

Citation for published version:
Cicione, A, Walls, R, Stevens, S, Sander, Z, Flores, N, Narayanan, V & Rush, D 2021, 'An experimental and numerical study on the effects of leakages and ventilation conditions on informal settlement fire dynamics', *Fire Technology*. https://doi.org/10.1007/s10694-021-01136-8

Digital Object Identifier (DOI):
10.1007/s10694-021-01136-8

Link:
Link to publication record in Edinburgh Research Explorer

Document Version:
Peer reviewed version

Published In:
Fire Technology

General rights
Copyright for the publications made accessible via the Edinburgh Research Explorer is retained by the author(s) and / or other copyright owners and it is a condition of accessing these publications that users recognise and abide by the legal requirements associated with these rights.

Take down policy
The University of Edinburgh has made every reasonable effort to ensure that Edinburgh Research Explorer content complies with UK legislation. If you believe that the public display of this file breaches copyright please contact openaccess@ed.ac.uk providing details, and we will remove access to the work immediately and investigate your claim.

Download date: 30. Jun. 2022

Title Page w/ ALL Author Contact Info.

An experimental and numerical study on the effects of leakages and ventilation conditions on informal settlement fire dynamics

Antonio Cicione
Stellenbosch University, Department of Civil Engineering, Stellenbosch, South Africa.

Richard Walls
Stellenbosch University, Department of Civil Engineering, Stellenbosch, South Africa

Sam Stevens
School of Engineering, University of Edinburgh, Edinburgh EH9 3JL, UK

Zara Sander
Stellenbosch University, Department of Civil Engineering, Stellenbosch, South Africa

Natalia Flores
Stellenbosch University, Department of Civil Engineering, Stellenbosch, South Africa

Vignesh Narayanan
Stellenbosch University, Department of Civil Engineering, Stellenbosch, South Africa

David Rush
School of Engineering, University of Edinburgh, Edinburgh EH9 3JL, UK

BLIND Manuscript without contact information Click here to view linked References

An experimental and numerical study on the effects of leakages and ventilation conditions on informal settlement fire dynamics

ABSTRACT

The one billion people that currently reside in informal settlements are exposed to a high and daily risk of large conflagrations. With the number of informal settlement dwellers expected to increase in the years to come, more systematic work is needed to better understand these fires. Over the past 3-4 years, researchers have explicitly started investigating informal settlement fire dynamics, by conducting full-scale experiments and numerical modelling research. It is with this background that this paper seeks to investigate the effects of leakages and ventilation conditions on informal settlement fire dynamics. Three full-scale informal settlement dwelling experiments were conducted in this work. The experiments were kept identical with only a small change to a ventilation or leakage condition from experiment to experiment. During each experiment the heat release rates, heat fluxes, temperature and flow data were recorded and are given in this paper. B-RISK's (a two-zone model software) predictive capabilities are then benchmarked against the full-scale experiments. B-RISK is then used to conduct a parametric study to further investigate the effects of leakages and ventilation on informal settlement dwelling fire dynamics. It was found that the ventilation conditions can significantly affect the radiation emitted from an informal settlement dwelling, and as a result increase or decrease the probability of fire spread to neighboring dwellings.

KEYWORDS: informal settlements, fire spread, enclosure fire dynamics, two-zone modelling.

1. INTRODUCTION

Despite the increase in informal settlement fire research and efforts for awareness, the number of informal settlement fire incidents are still increasing annually (e.g., in December 2019, Cape Town alone had 268 informal settlement fires, which is 23% more that in December 2018 [1]). Currently, there are approximately 1 billion people residing in informal settlements worldwide, and this number is expected to rapidly increase in the next 20-30 years [2]. With the number of informal settlement fires increasing annually, and since the number of informal settlement dwellers are expected to increase, there is a great need to better understand the factors that contribute towards large conflagrations in informal settlements on a fundamental level. Fig. 1 and Fig. 2 visually show typical informal settlement dwellings (ISDs) and an informal settlement, respectively, found in South Africa.

Fig. 1. Example of typical ISDs

Fig. 2. Informal settlement in Cape Town, South Africa

In the past few years, researchers have developed a preliminary understanding of informal settlement fire dynamics by applying early-stage Fire Dynamics Simulator (FDS) simulations to scenarios of interest, and by conducted preliminary fire spread experimental investigations. The first ISD experiments, were conducted by Walls et al. [3], where the study found that these makeshift dwellings behave similar to what one would expect of formal enclosures, i.e. informal dwellings experience ignition, a growth phase, flashover, a ventilation-controlled fully developed fire stage and a decay period (which is typically curtailed due to structural collapse for informal dwellings). Cicione et al. [4] continued the investigation of the informal settlement fire problem by conducting a series of full-scale experiments. Their experiments specifically focused on the effect of cladding materials on the internal fire dynamics and fire spread rates for informal settlements. The study further applied FDS to specific scenarios of the experiments conducted and from the simulation results it was found that dwellings spaced at approximately 3 m are not susceptible to fire spread (in 'still' wind conditions). This finding is similar to that found by Wang et al. [5] and Cicione et al. [6] where they estimated the critical separation distance between dwellings for fire spread not to occur, under still wind conditions, to be approximately 3-4 m. Beshir et al. [7] conducted a numerical investigation (using FDS) on the effect of horizontal roof openings on the internal fire dynamics of ISDs as well as on the heat fluxes emitted by these dwellings. They found that dwellings with a horizontal roof vent had a slower time to flashover and emitted lower heat

fluxes to its surroundings. Beshir et al. [8] continued the numerical investigation of vents (using FDS), with the focus shifted to the effect of vertical opening positions with respect to a door opening. It was found that the position of a vertical opening with respect to a door opening also has an effect on the heat fluxes emitted. Cicione et al. [9,10], looked at the possibility of simulating informal settlement fire spread using a semi-probabilistic approach. Although, the method showed real potential, a number of variables are still unknown that are needed to further develop the proposed method. One of these unknown variables is the effect of ventilation conditions on the radiation emitted by an ISD, which is investigated in the paper. Wang et al. [11] looked at the effect of ventilation conditions on ISD fire dynamics (dwelling scale), in laboratory conditions. Research relating to ISD fires is relatively immature and therefore there is a paucity of specific literature called upon above.

The research mentioned above has provided a basis for informal settlement fire dynamics, but there is still a significant need to answer specific questions on a more fundamental level. It is with this in mind that this paper seeks to answer a very specific question: How do leakages and ventilation conditions effect informal settlement (both on a settlement and dwelling scale) fire dynamics?

2. EXPERIMENTAL SET-UP

In December 2019, a series of full-scale informal settlement fire experiments were conducted at Breede Valley Fire Department, in Worcester, South Africa. In this work, only 3 of the 9 experiments are discussed. As mentioned above, the focus of this paper is on the effect of leakages and ventilation conditions on ISD fire dynamics, hence only the experiments contributing towards better understanding these effects are included here. From the other six experiments, two experiments focused on the effect of separation distance on fire spread can be found in Cicione et al. [12]; three experiments investigated the effect of different lining materials on the fire spread rates and internal fire dynamic; and one experiment was a double storey informal settlement dwelling, another experiment looked at the effect of internal divisions on the ISD fire dynamics. The general experimental setup of the 3 experiments considered in this work is identical, as depicted in Fig. 3. All experiments consisted of two dwellings denoted ISD1 (left dwelling in Fig. 3) and ISD2 (right dwelling in Fig. 3).

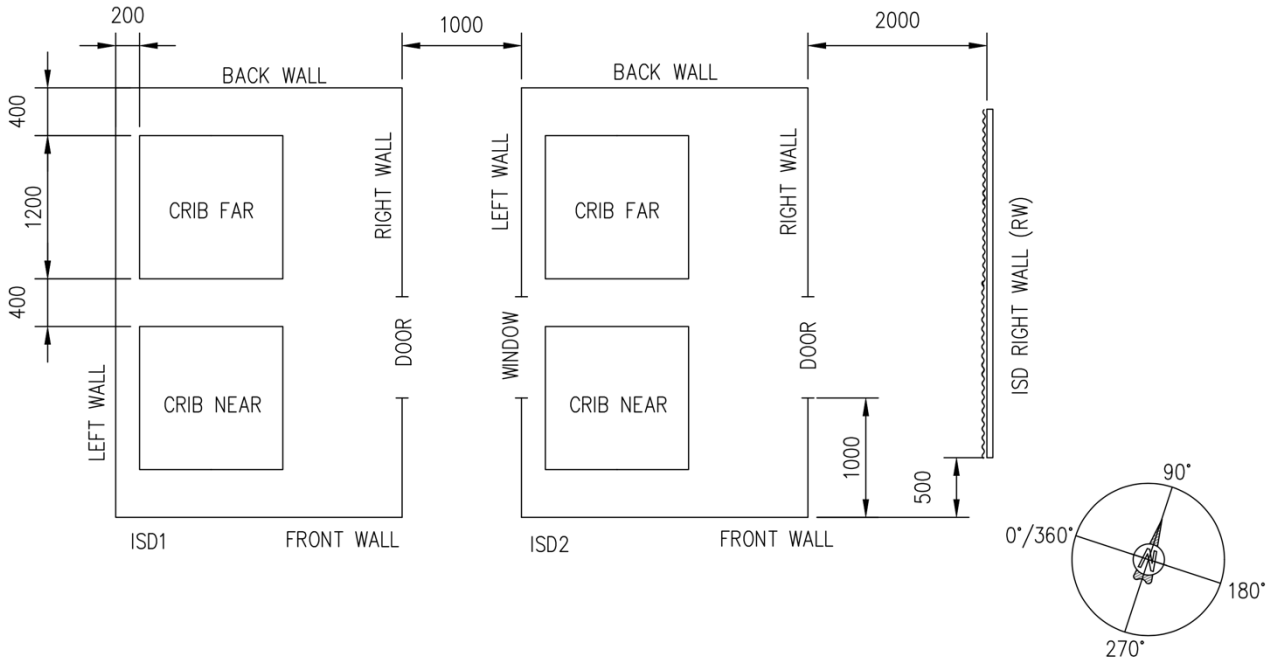

Fig. 3. Experimental setup, with ISD1 being the dwelling of origin, the fire spreading to ISD2. Units are in mm.

In all experiments, the dwelling on the left in Fig. 3 was the dwelling of fire origin and is denoted as ISD1 for the remainder of the paper. The fire was then left to spread from ISD1 to the target dwelling, the dwelling on the right of Fig. 3, and is denoted as ISD2. All experiments had the exact same general setup, but for each experiment ISD2 had a change in its ventilation- or leakage condition. ISD1 was ignited by igniting 8 small bags, filled with a 400 mm × 400 mm of kerosene dipped hessian, with one bag placed at each of the bottom 4 corners of each crib (similar to what was done in [11,12]). A lone standing wall was setup, upon which heat fluxes were measured, and is referred to as ISD Right Wall (denoted as RW), as depicted in Fig. 3.

2.1. Design of dwellings

All dwellings used in these experiments had a floor area identical to that of the ISO 9705 room (3.6 m×2.4 m), and were 2.3 m in height, similar to those used in previous ISD research [3,11,13–15]. Since informal dwelling construction methods and materials have been discussed in detail by numerous researchers, it is not included here. However, should the reader require more information regarding informal dwelling construction materials etc. the reader should refer to refs. [3,11,13–15]. For all experiments, ISD1 was clad with IBR (inverted box rib) sheeting that was fixed to a steel frame. Steel sheeting, which is typically galvanized, is one of the most common cladding materials used in informal settlements [3,14]. In order to reproduce a consistent fire scenario in ISD1, such that all 3 experiments had a similar fire in ISD1, the dwelling only had one opening, a door with an internal dimension of 2.05 m (height) × 0.85 m (width), no cardboard lining (as one would typically find in an ISD [3,11,13–15]) and all openings created by the flutes of the IBR sheets (38 mm flute height) were closed with ceramic blanket (in reality the openings created by flutes are often left open, stopped with clay or even combustible materials such as newspaper). For all experiments, ISD2 was clad with corrugated steel sheets, that were fixed to SA pine timber frames (50 mm × 50 mm) with an approximate density of 450 kg/m^3, and were lined with cardboard mimicking the highly flammable lining and contents present in many real ISDs [6]. ISD2 had two openings: (1) a window opening with an internal dimension of 0.6 m (height) × 0.85 m (width), with the windowsill placed 1.25 m from ground level, and (2) a door opening with an internal dimension of 2.05 m (height) × 0.85 m (width). Specific details of the experiments are:

1. For the first experiment (denoted as Exp 1), all openings created by the flutes of ISD2 (18 mm flute height, which is different to ISD1 due to the profile used) were closed with ceramic blanket to simulate a fire scenario with 'no leakages' (Fig. 4).
2. For the second experiment (denoted as Exp 2), all openings created by the flutes of ISD2 were left open to simulate a fire scenario with leakages (Fig. 5). The hypothesis was that leakages will increase fire spread rates since the openings allowed for flame impingement, but might reduce the radiation emitted since more hot gases are allowed to escape the enclosure.
3. Lastly, the third experiment (denoted as Exp 3), was an exact replica of Exp 1, but had a glass pane installed at the window (Fig. 6), and the back 1.4 m × 2.4 m area (relative to Fig. 3) of the roof had polycarbonate sheets (Fig. 6), as opposed to steel sheets. Since the polycarbonate sheets have a low melting point (of approximately 155°C), the polycarbonate sheets will melt as ISD2 ignited, creating a horizontal roof vent. The hypothesis was that as soon as the polycarbonate sheets melted away, the additional ventilation would reduce the external flames from the door opening, which would reduce the likelihood of fire spread. This is building on a concept first introduced by Beshir et al. [16]. Here the effects of both a glass window and polycarbonate sheets are investigated. It is assumed that the window will not affect results for the polycarbonate sheets and vice versa. Since the glass window will only affect the fire behavior up to ignition of ISD 2 and the polycarbonate sheets will only affect the fire behavior once ISD2 is ignited.

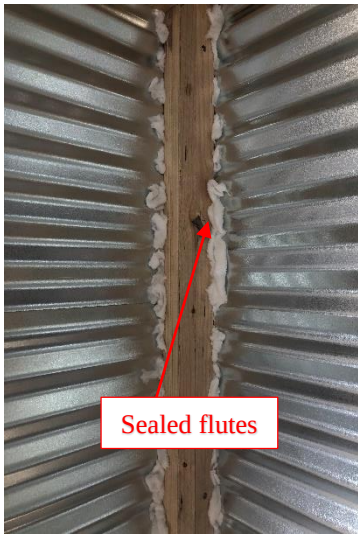

Fig. 4. Closed flutes in ISD2 for Exp 1

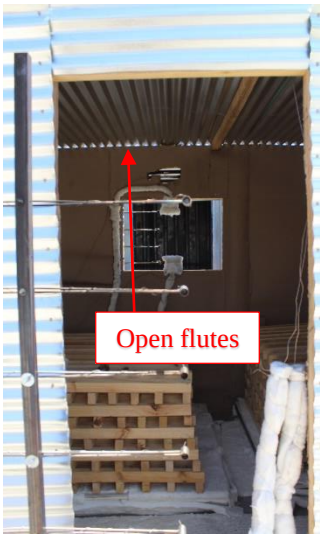

Fig. 5. Open flutes in ISD2 for Exp 2

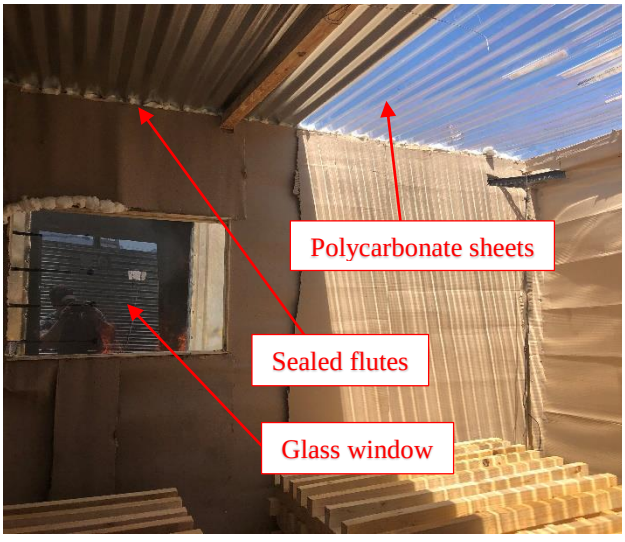

Fig. 6. Polycarbonate sheets and glass window inside ISD2 during Exp 3

Table 1 summarizes the parameters pertaining to ISD2 for the three full-scale experiments considered in this work. ISD1 was exactly the same for all three experiments.

Table 1: Summary of the ISD2 used in full-scale experiment conducted in this work

	Experiment 1 (Exp 1)	**Experiment 2 (Exp 2)**	**Experiment 3 (Exp 3)**
Wall material	Corrugated steel sheets	Corrugated steel sheets	Corrugated steel sheets
Lining material	Cardboard	Cardboard	Cardboard
Leakages (Open flutes)	No	Yes	No
Roof vent	None	None	1.4 m × 2.4 m
Glass in window	No (window open)	No (window open)	Yes (3 mm thick)

2.2. Fuel

In reality the fuel load in informal settlement dwellings can range significantly and according to Walls et al. [3], the fuel load can be anything from 400 MJ/m^2 to 2000 MJ/m^2, but this requires further research to be accurately defined. Cicione et al. [6] interviewed a number of firefighters, that fought more than 2000 informal settlement fire combined. These firefighters estimated that the fuel load in ISDs is higher than that of formal dwellings (an average of 780 MJ/m^2) as stipulated in the EN1991-1-2 [17]. For simplicity and experimental purposes, it was decided to make the fuel load 30 kg/m^2 of timber, that had a calorific value of 17 MJ/kg as measured by the bomb calorimeter, resulting in a fuel load of approximately 510 MJ/m^2. The 200 timber pieces (0.04 m ×0.06 m × 1.2 m) were divided into two timber cribs. Each crib had 10 layers with 10 timber pieces per layer (Fig. 5 and Fig. 6). Using ref. [18], it was estimated that for free burning conditions, these cribs would have a surface-controlled mass loss rate (MLR) limit of 0.39 kg/s combined. However, for burning within an enclosure, the ventilation-controlled MLR is calculated using the following equation [19]:

$$\dot{m} = 0.12 A_o \sqrt{H_o} \quad (1)$$

where A_o is the total area of the openings and H_o is the area-weighted equivalent opening height. For ISD1 and ISD2 the calculated ventilation-controlled MLRs are 0.3 kg/s and 0.355 kg/s (i.e., without accounting for the roof vents or leakages), respectively. The cribs were placed 200 mm from the left long wall of each dwelling, 400 mm from the short walls and 400 mm apart, as depicted in Fig. 3. As mentioned earlier, ISD1 had no cardboard lining for all 3 experiments, but ISD2 had cardboard lining for all experiments (Fig. 5 and Fig. 6) in order to mimic the highly flammable cladding and contents present in many real ISDs [6].

2.3. Measurements

All gas temperatures were recorded using 1.5mm diameter Type K thermocouples (TCs). The incident heat fluxes emitted by the dwellings were captured using Thin Skin Calorimeters (TSCs), that were calibrated against a water-cooled heat flux gauge. Both the TSC and TC readings were recorded with an Agilent 34980A data logger at a frequency of 0.2 Hz. The external reference temperature was recorded with a 4-wire resistance temperature detector (RTD). Flow velocities were measured at the door and window openings using Bi-directional Flow Probes (FPs) and MLRs were recorded for each timber crib by placing each crib on a 1.2 m × 1.2 m scale with a 10 g accuracy. Wind speed and direction were measured using a hemispherical cup-type anemometer, placed approximately 10 m away from the experimental setup at a height of 2 m. All voltage output data was recorded at a frequency of 1 Hz. Fig. 7 depicts the positions of all TSCs, TCs, FPs and scales. The number next to the instrumentation abbreviation indicates the number of instruments in a particular equipment tree (e.g., TCx, where x is the number of TCs at that position). Fig. 8 depicts the spacing of each equipment tree used in these experiments.

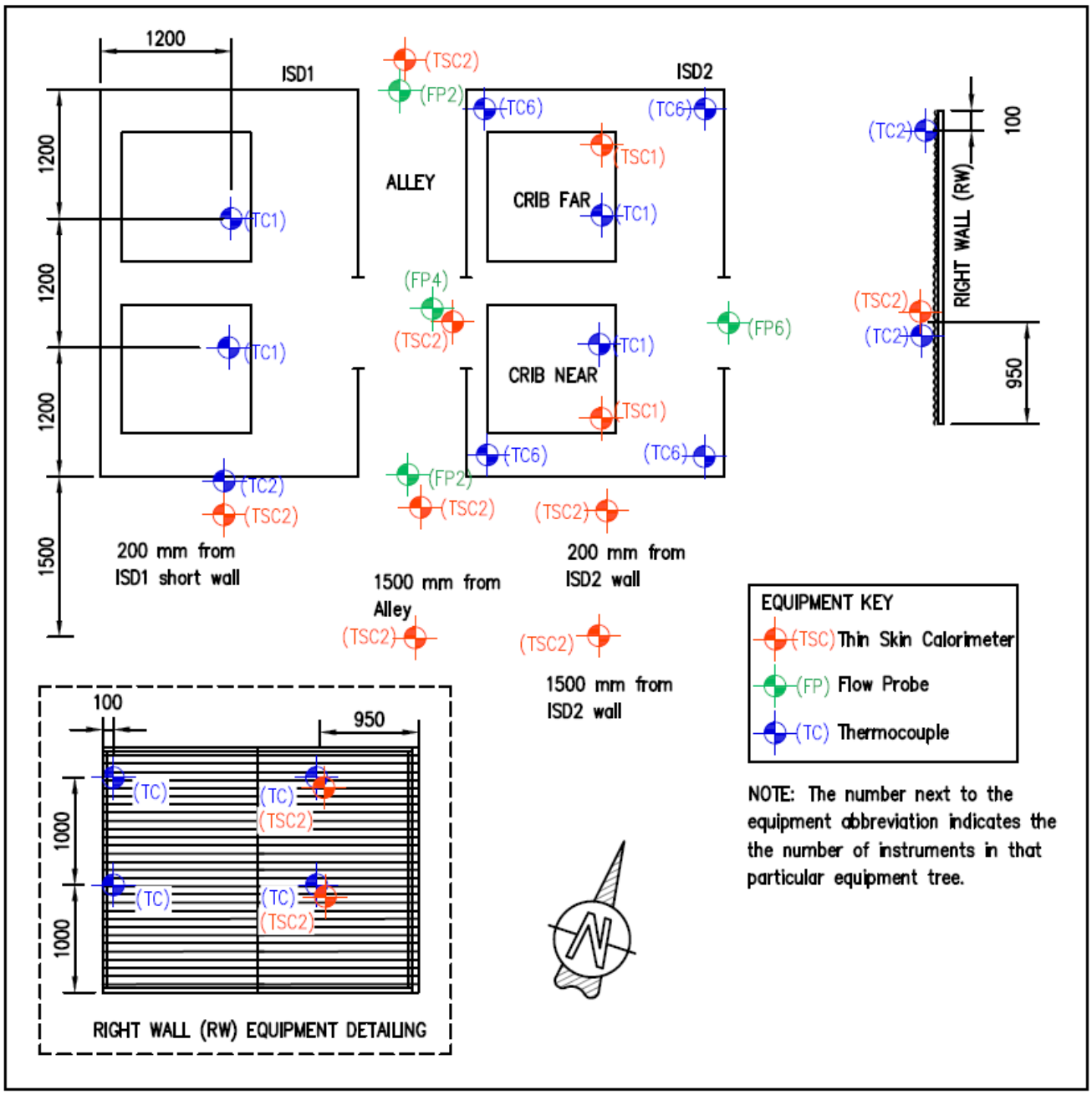

Fig. 7. Equipment layout (top), equipment key (middle right), and right wall detailing (bottom left)

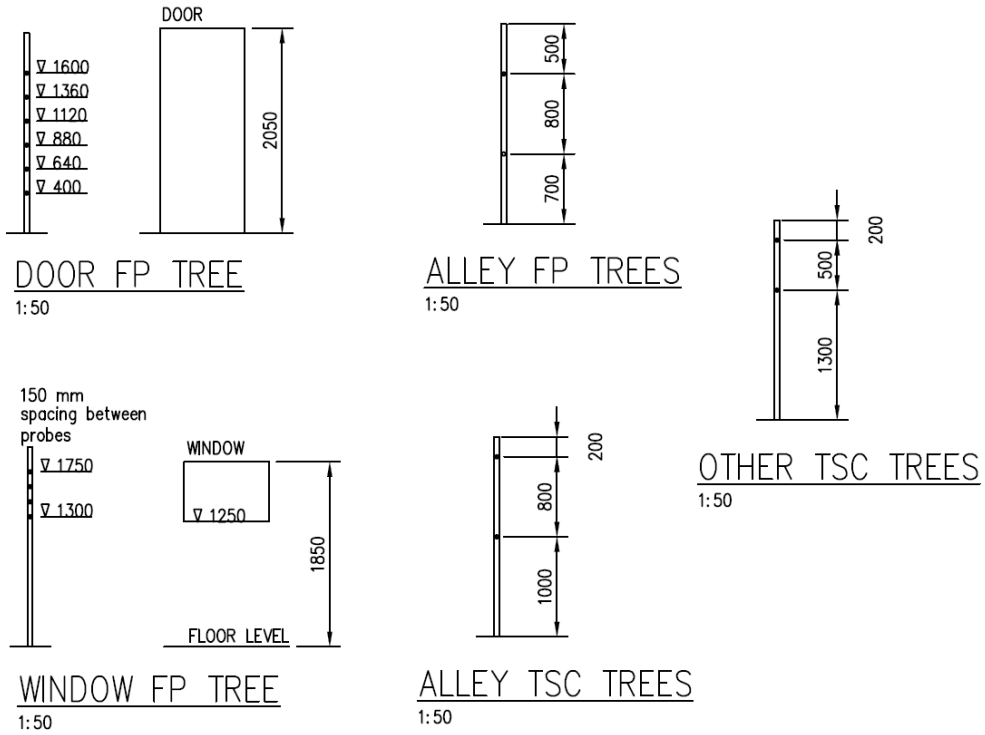

Fig. 8. Instrumentation heights for the various equipment trees

3. B-RISK SETUP OF EXPERIMENTS CONDUCTED

In this work, B-RISK [20], a two-zone model software, is used to simulate the experiments conducted and to further investigate the effect of leakages and ventilation on ISD fire dynamics through a parametric study. In this section the simulation setup of the three experiments conducted, denoted as Exp 1, Exp 2 and Exp 3, are discussed. The numerical results are presented alongside the experimental results in the sections that follow. Only ISD2 was simulated in B-RISK for each experiment, since the ventilation or leakage changes only occurred in ISD2, with ISD1 being exactly the same for all three experiments. The ISD2 dwelling size was used for the volumetric domain size in B-RISK ("Room Design" in B-RISK), and the combustion properties used for the timber cribs (simulated as an item under "Fire Specification" in B-RISK) were those noted in section 2.2 above. Cardboard lining was ignored since it only contributed towards the fire for a few seconds (discussed below) and only the mass loss rates of the cribs was measured in the experiments. A soot yield of 0.015 g/g, CO2 of 1.33 g/g and radiant loss fraction χ_R of 0.3 were taken from Table 3-4.14 of the SFPE Handbook [21]. The heat of gasification (1.8 kJ/g) has been selected from Table 3-4.7 of the SFPE Handbook [21], based on similar representative materials. Assuming a combustion efficiency of 1, the effective heat of combustion equals the gross heat of combustion (17 kJ/g) of the timber used in these experiments. All sheets were assumed to be flat in B-RISK since corrugated sheets cannot be simulated in B-RISK. Additionally, leakages created by the corrugated flutes (Exp 2) were assumed to be regular openings with the same opening size as in the experiment, located at the top of the walls (i.e., assuming the flute opening to be 9 mm high in B-RISK). A summary of the inputs to the B-RISK scenarios are listed in Table 2.

Table 2: Summary of B-RISK inputs

Model Name	Corresponding Experiment	Heat release rate curve used	Ventilation and Geometry details
Scenario 1	Exp 1	HRR curve of Exp 1 as depicted in Fig. 13 b)	The exact geometry and ventilation conditions as described in Fig. 3, Fig. 4 and Table 1
Scenario 2	Exp 2	HRR curve of Exp 2 as depicted in Fig. 13 b)	The exact geometry and ventilation conditions as described in Fig. 3, Fig. 5 and Table 1
Scenario 3	Exp 3	HRR curve of Exp 3 as depicted in Fig. 13 b)	The exact geometry and ventilation conditions as described in Fig. 3, Fig. 6 and Table 1

Since B-RISK is a zonal model software, external wind conditions cannot be simulated (this is one limitation of zone modelling), hence wind was not simulated in any of the B-RISK scenarios.

4. EXPERIMENTAL RESULTS AND DISCUSSION

For Exp 1 (no leakages – i.e. closed flutes), depicted in Fig. 9 a) and b), ISD1 reached a fully developed fire stage within 3.9 minutes after ignition. At this point, flames emerged out of the door, pushing hot gases into ISD2. From a water-cooled camera placed within ISD2, one could see flames pulse through the window every few seconds. Seconds before the ignition of ISD2, the gas temperature of the hot layer inside ISD2 reached a uniform temperature of approximately 164-174 °C from ceiling level to approximately 2.05 m from ground level (this is the height of the door). At approximately 5.4 min the cardboard lining (above the window) of ISD2 ignited, and as a result of the preheating, rapid fire spread across the surface of the cardboard ensued horizontally, then down, leading to flashover and a fully developed stage that was attained within 1.5 minutes. Note that flashover in this paper refers to a rapid transition period between the growth phase and the fully developed phase, as opposed to a single point of transition.

Fig. 9 a) Visually depiction of Exp 1

Fig. 9 b) Inside view through the door of ISD2 for Exp 1

For Exp 2 (leakages – i.e. open flutes), depicted in Fig. 10 a), ISD1 reached a fully developed fire stage within 3.9 minutes. At this point, flames already emerged out of the door, pushing hot gases into ISD2. From a water-cooled camera inside ISD2, one could see flame pulse through the window every few seconds, as per Exp. 1. Seconds before the ignition of ISD2 the gas temperature of the hot layer inside ISD2 reached a uniform temperature of approximately 90-115 °C from ceiling level to approximately 2.05 m from ground level. At approximately 5.3 min the cardboard lining of ISD2 ignited (Fig. 10 b)), and as a result of the preheating, rapid fire spread across the surface of the cardboard ensued (horizontally, then vertically down), leading to flashover and a fully developed stage that was attained within 2 minutes.

Fig. 10 a) Visually depiction of Exp 2

Fig. 10 b) Ignition of the cardboard lining in ISD2 for Exp 2

For Exp 3 (roof vent), after ignition, ISD1 reached a full developed fire stage within 4.2 minutes. At this point, flames already emerged out of the door, pushing hot gases into ISD2. From video footage inside the door of ISD2, one could see the glass window cracking at about 3 minutes (from ignition of ISD1), partial fallout at about 3.5 minutes and complete fallout at approximately 8 minutes (although complete fallout is difficult to visually identify in the video footage). Seconds before the ignition of ISD2 the gas temperature of the hot layer inside ISD2 reached a uniform temperature of approximately 50 °C from

ceiling level to approximately 2.05 m from ground level. At approximately 5 minutes the cardboard lining of ISD2 ignited. The heat from the burning cardboard rapidly melted the polycarbonate sheets as depicted in Fig. 11 a) to d). A fully developed stage was attained within approximately 3.7 minutes after ignition.

Fig. 11 a) Ignition of ISD2

Fig. 11 b) Early spread of flames across the cardboard surface and the polycarbonate sheets starting to melt

Fig. 11 c) Visual illustration of the melting of the polycarbonate sheets

Fig. 11 d) Polycarbonate sheets almost completely melted away

Table 3 summarizes the details pertaining to ignition, flashover and flame spread for Exp 1 – Exp 3 as discussed above.

Table 3: Summary of Exp 1 - Exp 3. Note that the percentages in brackets show the percentage increase (+) or decrease (-) compared to Exp 1.

	Exp 1 (closed flutes)	**Exp 2 (Open flutes)**	**Exp 3 (Glass window – polycarbonate roof sheets)**
Ventilation	Open door and window (flutes closed)	Open door, window and flutes	Open door. Glass window. Polycarbonate sheets roof (flutes closed)
Time to fully developed fire stage in ISD1 [minutes]	3.9	3.9 (0%)	4.2 (+7.7%)
Hot layer temperature prior to ignition of ISD2 [°C]	164-174	90-115 (-45%)	45-50 (-73%)
Time-to-ignition of ISD2	5.4	5.3 (-1.85%)	5.0 (-7.4%)

[minutes]			
Ignition to fully developed stage in ISD2 [minutes]	1.5	2 (+33%)	3.7 (+147%)
Average HRR of ISD2 for the first 2 minutes after the fully developed fire stage was reached [MW]	6.2	7.2 (+16%)	8.7 (+40%)
Average heat flux to the top of the RW over any 2 minutes that gives the highest average (before structural collapse) [kW/m^2]	38	39 (+2.6%)	31 (-18%)
Maximum incident heat flux on to RW [kW/m^2]	52	59 (+13%)	39 (-25%)
Maximum horizontal flame length from door opening (based on video footage) [meters]	2.2 m	2 m (-9%)	0.2-0.4 m (-82%)

Based on the data in Table 3, it is clear that the glass window panel and open or closed flutes had no effect on the fire spread rate for this experimental configuration (door to window fire spread), as the window opening was dominant in controlling fire spread. Once ISD2 ignited, the ventilation clearly had a substantial effect on the time to flashover. Exp 1 had the least openings and thus experienced the largest amount of heat buildup with a hot layer temperature of approximately 164-174°C in ISD2, prior to ignition. Exp 2 experienced almost exactly the same time to flashover as Exp 1, even with open flutes. However, the hot gases were able to escape more easily, resulting in a slightly lower hot layer temperature of around 90-115°C in ISD2, prior to ignition. The glass installed in ISD2 for Exp 3 significantly reduced the amount of hot gases entering ISD2 and, as a result, the hot gas layer temperature in ISD2 was below 50°C prior to ignition. From the video data, it is clear that fire spread rate across the surface of the cardboard lining were faster for the experiments where the hot layer temperature was higher prior to ignition. Although obvious, it shows that dwelling configurations with less ventilation at ceiling level will trap the hot gases better, which will increase that rate at which the lining material preheats, allowing for faster fire spread across the cardboard lining, that as a result, leads to the onset of flashover occurring faster. Additionally, an enclosure with lower ventilation would require a lower HRR for flashover to occur [22]. Hence, less ventilation increases the spread rate over the surface of the lining material and at the same time reduces the HRR needed for the onset of flashover.

Fig. 12 a) to c) depict the wind direction and wind speed during Exp 1 to Exp 3, respectively. A wind direction of 0° indicates an east wind with a clockwise rotation being positive (Fig. 3). The wind data was captured approximately 10 m away from the experiments (to exclude fire-induced flows from the measurements), towards the bottom left corner of Fig. 3, at a height of 2 m using a hemispherical cup-type anemometer.

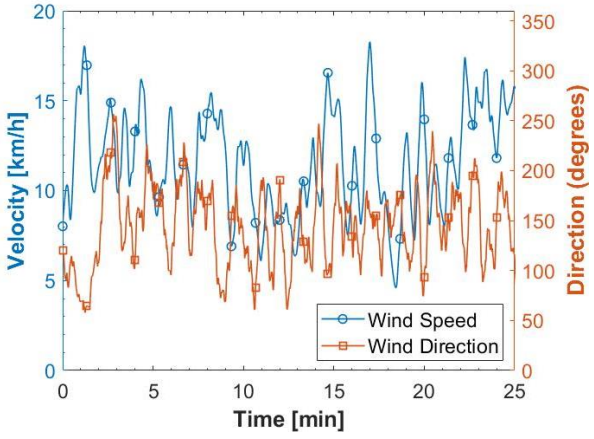

Fig. 12 a) Wind speed and direction during Exp 1

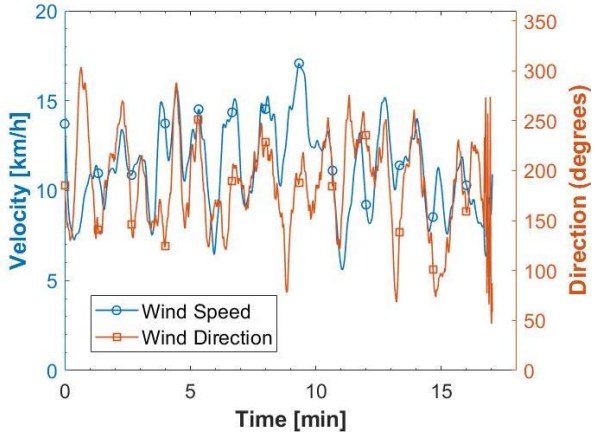

Fig. 12 b) Wind speed and direction during Exp 2

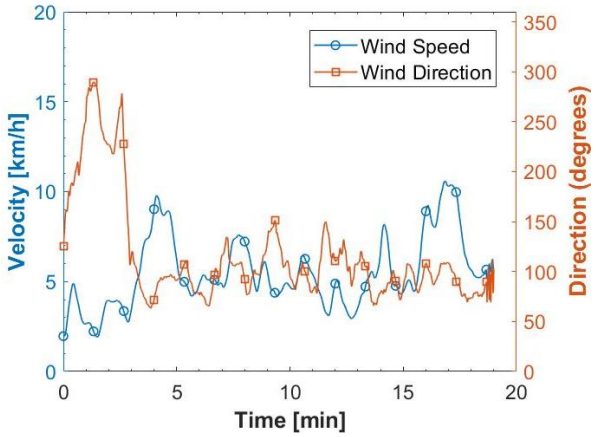

Fig. 12 c) Wind speed and direction during Exp 3. A wind direction of 0° indicates an east wind with a clockwise rotation being positive.

4.1. Heat release rates

Fig. 13 a) and b) depict the heat release rates of ISD1 and ISD2 for Exp 1 to Exp 3, respectively, based on the MLR from the scales. For the positioning of the scales refer to Fig. 7.

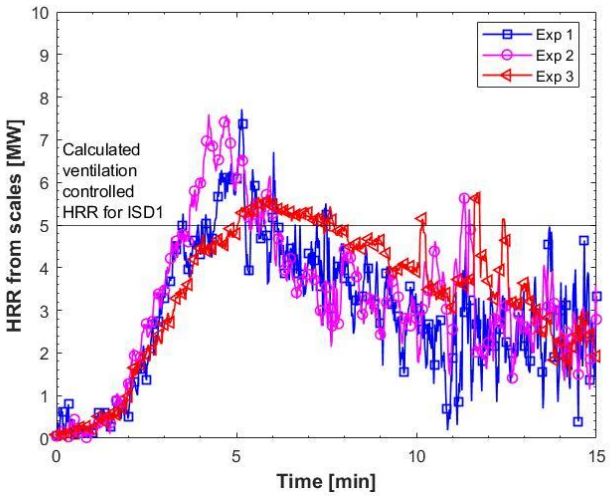

Fig. 13 a) HRRs of ISD1 as indirectly measured by the scales

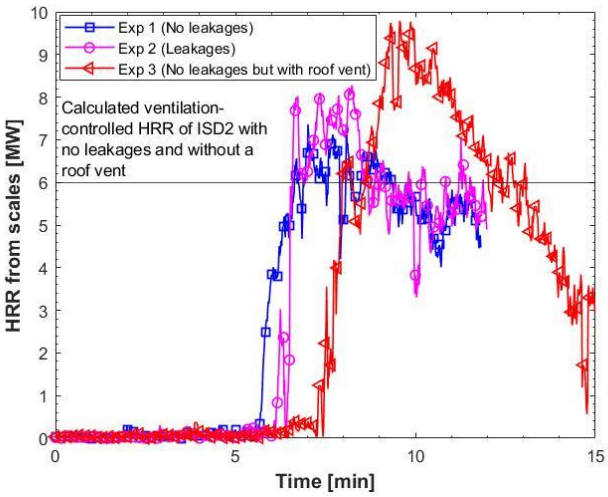

Fig. 13 b) HRRs of ISD2 as indirectly measured by the scales

For ISD2 (Exp 3), the polycarbonate sheets created a large opening meaning that the enclosure was not ventilation-controlled and that the mass loss rates of the cribs should be limited by the crib geometry. According to Babrauskas [23] the mass loss rate of a free burning crib can be either porosity-controlled or surface-controlled. The HRR of the free burning cribs can then be estimated by the following very well-known HRR formula:

$$\dot{Q} = \dot{m}\Delta H_{eff} \tag{2}$$

where $\dot{m}$ is the mass loss rate [kg/s] and ΔH_{eff} is the effective heat of combustion [kJ/kg]. The mass loss rate, i.e. of the free burning cribs, is taken as the lesser of the surface-controlled mass loss rate:

$$\dot{m} = \frac{4}{D} m_0 v_p \left(1 - \frac{2 v_p t}{D}\right) \tag{3}$$

and porosity-controlled mass loss rate:

$$\dot{m} = 4.4 \times 10^{-4} \left(\frac{S}{h_c}\right)\left(\frac{m_0}{D}\right) \tag{4}$$

where the stick thickness is D = 0.04 m, the clear spacing is S = 0.09 m, the crib height is h_c = 0.6 m, the number of sticks per row is n = 10, the initial crib mass was m_0 = 130 kg, giving $v_p = 2.2\times10^{-6}D^{-0.6}$ according to Babrauskas [19] and the heat of combustion of the timber is $\Delta Heff$ = 17 MJ/kg (as measured by a bomb calorimeter test and assuming a combustion efficiency of 1). In this case, there were 2 cribs, thus the mass loss rate is multiplied by 2 to give the total HRR. Substituting all the knowns into Equation 3 and Equation 4, the porosity-controlled HRR is calculated as 7.2 MW and the surface-controlled HRR is calculated as 6.7 MW. Implying that the free burning crib will have an absolute maximum HRR, that is surface-controlled, of 6.7 MW. However, in Fig. 13 b) it is clear that the HRR of the cribs exceeded the surface-controlled HRR and even

exceeded the porosity-controlled HRR. This is most likely because for Exp 3 we have forced flow through the cribs due to air entrainment, i.e. higher velocities than normal created by a so called 'chimney effect'. This is evident when we consider the inward gas velocities measured by the door flow probes. For Exp 1 and 2, the maximum inward gas velocity is approximately 2 m/s, where the maximum inward gas velocity for Exp 3 is approximately 4 m/s. This is discussed in more detail in the sections that follow.

Considering Exp 1, it can be seen that the calculated surface-controlled HRR of the cribs of approximately 6.7 MW, corresponds relatively well with the total MLR measured by the scale. The maximum measured HRR is approximately 7.6 MW for ISD1 and 7.2 MW for ISD2. Equation 1 gives a ventilation limited fire of about 6 MW within the dwelling. The remaining energy release rate, $7.6 - 6 = 1.6$ MW for ISD1 and $7.2 - 6 = 1.2$ MW for ISD2, must then burn outside of the dwellings. This is clear when comparing the flame lengths of ISD1 and ISD2 (Fig. 9). From video footage, it is clear that a large volume of flames emerges from ISD1 compared to ISD2, as depicted in Fig. 9.

4.2. Gas temperatures

Fig. 14 a) to d)Fig. depict the temperature profile across the height of ISD2 for Exp 1 and the B-RISK scenario 1 (scenario 1 corresponds to Exp 1) at the left back, right back, right front and left front, respectively. The thermocouples were labelled from TC6 to TC1, with TC6 being at the top and TC1 being at the bottom of the TC tree. The TCs were placed at the following heights, from floor level, for each tree: 2.2 m, 2.15 m, 2.05 m, 1.9 m, 1.7 m and 1.55 m. The reason the thermocouples were more concentrated in the top part of the dwelling was because the authors were interested in the smoke layer development before flashover to understand the preheating in the second dwelling. These graphs are only plotted up to structural collapse, which occurred at approximately 12.4 minutes after ignition of ISD1. As mentioned earlier, during Exp 1, seconds before ignition of ISD2 the gas temperature of the hot layer inside ISD2 reached a uniform temperature of approximately 164-174 °C from ceiling level to approximately 2.05 m from ground level (this is the height of the door).

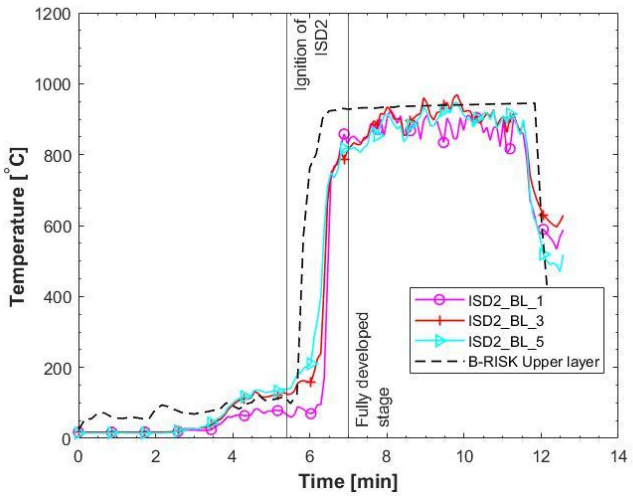

Fig. 14 a) Back left thermocouple tree of ISD2 for Exp 1 and B-RISK

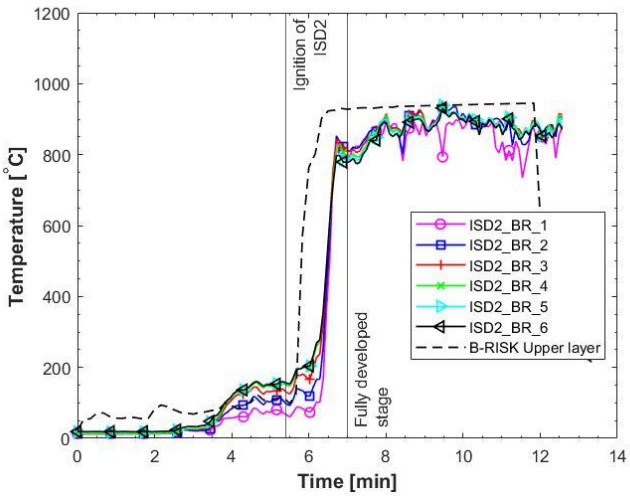

Fig. 14 b) Back right thermocouple tree of ISD2 for Exp 1 and B-RISK

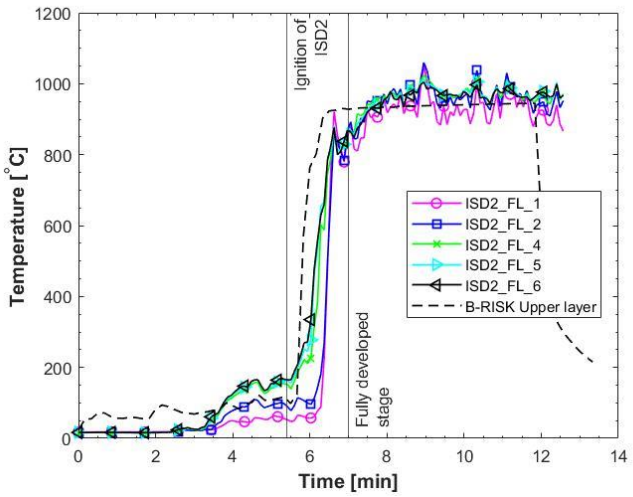

Fig. 14 c) Front left thermocouple tree of ISD2 for Exp 1 and B-RISK

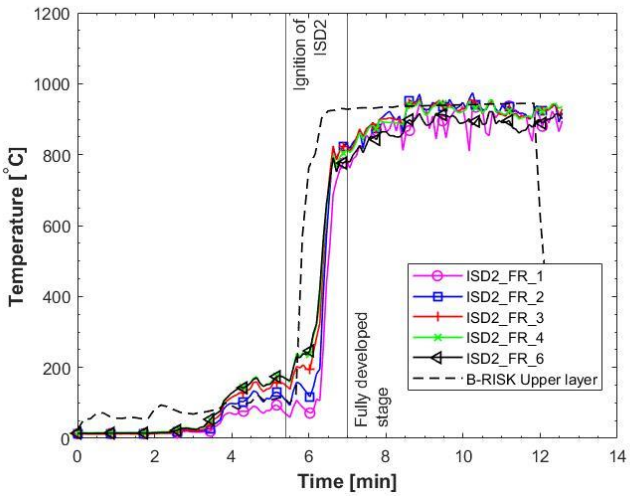

Fig. 14 d) Front right thermocouple tree of ISD2 for Exp 1 and B-RISK

Fig. 15 a) to Fig. d) depict the temperature profile across the height of ISD2 for Exp 2 and the B-RISK scenario 2 at the left back, right back, right front and left front, respectively. The thermocouples were labelled and spaced the same as Exp 1. Similar to Exp 1, the graphs are only plotted up to structural collapse that occurred at approximately 12.4 minutes after ignition of ISD1 (which just happens to be the same as Exp 1).

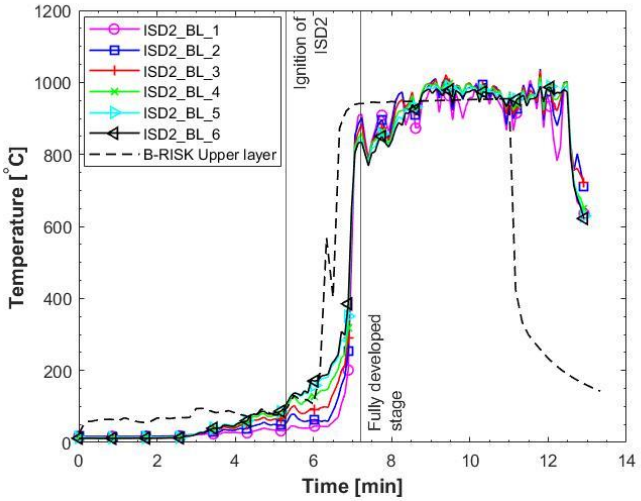

Fig. 15 a) Back left thermocouple tree of ISD 2 for Exp 2 and B-RISK

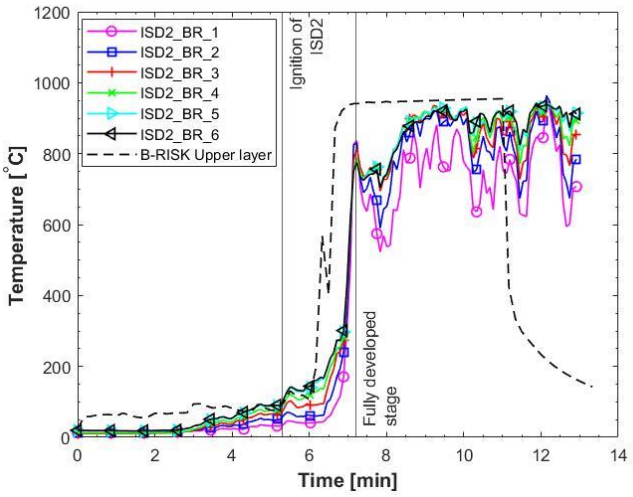

Fig. 15 b) Back right thermocouple tree of ISD 2 for Exp 2 and B-RISK

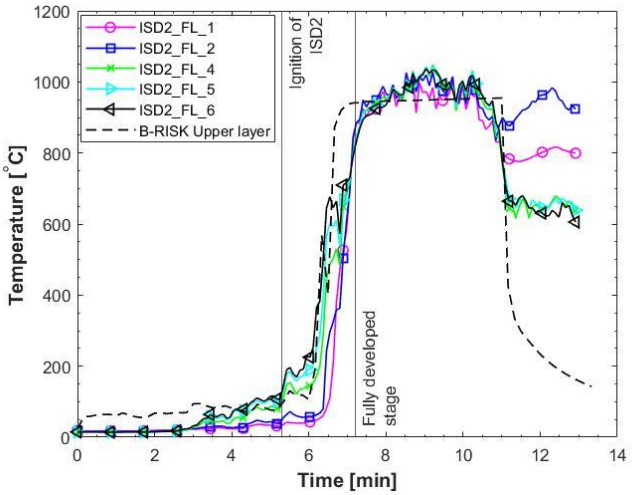

Fig. 15 c) Front left thermocouple tree of ISD 2 for Exp 2 and B-RISK

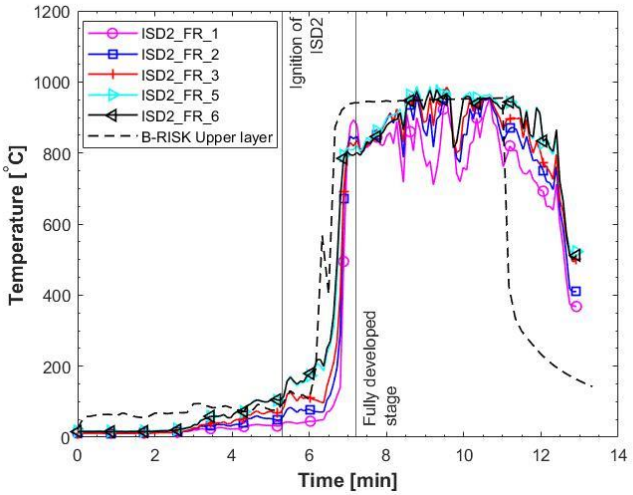

Fig. 15 d) Front right thermocouple tree of ISD 2 for Exp 2 and B-RISK

Fig. 16 a) to d)Fig. depict the temperature profile across the height of ISD2 and the B-RISK scenario 3 at the left back, right back, right front and left front, respectively. The thermocouples were labelled and spaced the same as Exp 1 and Exp 2. These graphs are only plotted up to structural collapse that occurred at approximately 16 minutes after ignition of ISD1.

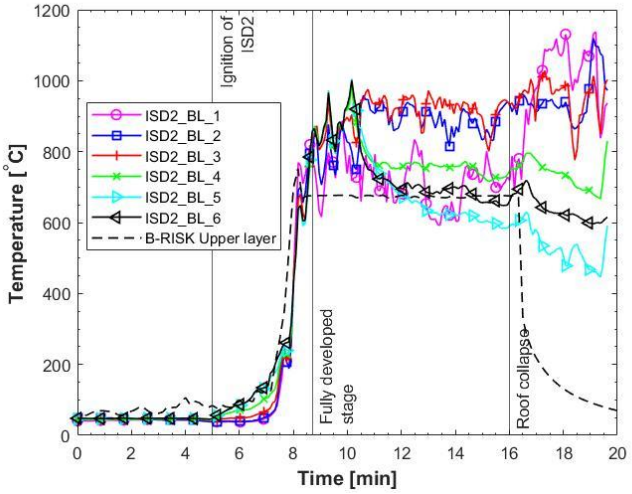

Fig. 16 a) Back left thermocouple tree of ISD 2 of Exp 3 and B-RISK

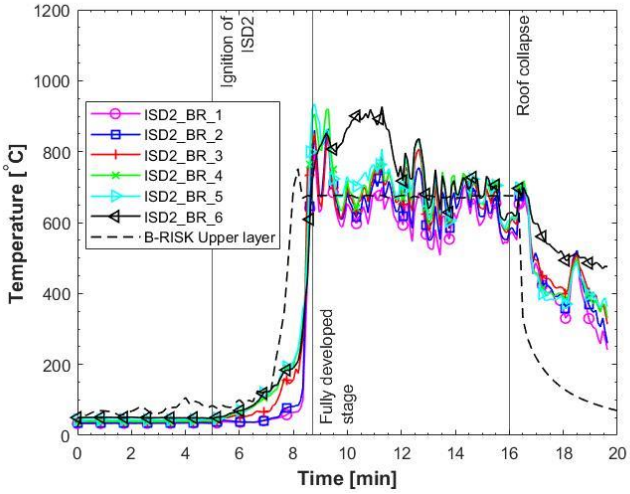

Fig. 16 b) Back right thermocouple tree of ISD 2 of Exp 3 and B-RISK

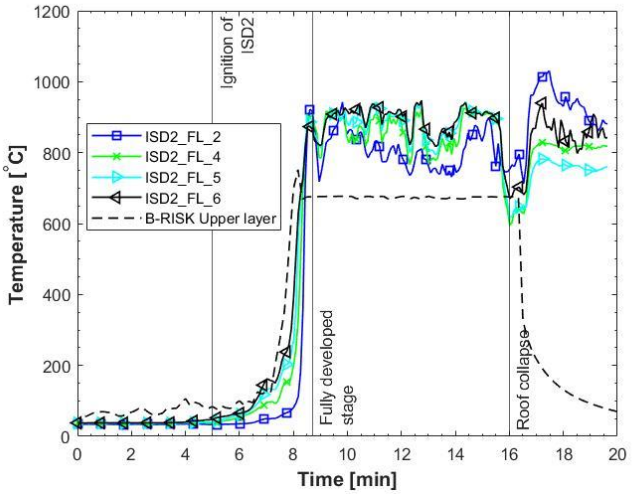

Fig. 16 c) Front left thermocouple tree of ISD 2 of Exp 3 and B-RISK

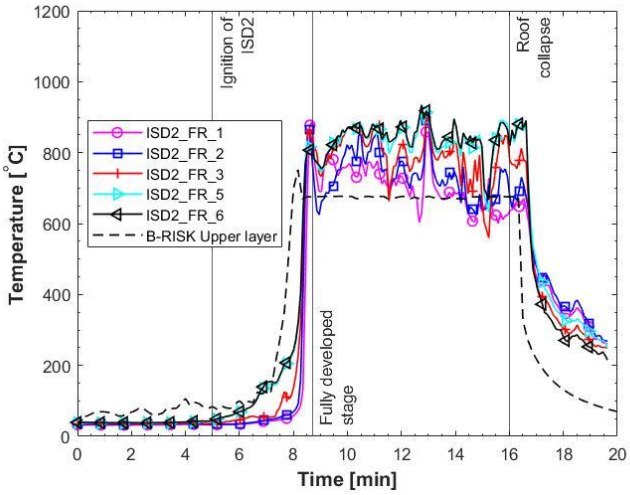

Fig. 16 d) Front right thermocouple tree of ISD 2 of Exp 3 and B-RISK

Considering Fig. 14 to Fig. 16, it is clear that B-RISK captures the time-temperature development within these dwellings sufficiently well. It appears that B-RISK slightly underpredicts the time to flashover for these dwellings, with the deviation in time to flashover being less than 10% in all cases. The maximum temperatures reached during the fully developed stage are very similar to that expected for formal dwellings of just below 1000 °C on average for Exp 1 and Exp 2 and around 600-800 °C for Exp 3 (depending if one considers the front or back temperatures). The maximum temperatures are captured extremely well by B-RISK with the only significant deviations being in Exp 3 at the front of the dwelling. It should be noted that for this zone model only the area of the roof vent is accounted for and not the location of the roof vent. The gas temperatures are then averaged out across the hot layer (upper layer in B-RISK). Hence, B-RISK captures the temperature relatively well at the back ISD2 for Exp 3, where the vent was actually located, but does however miss the slight heat build-up at the front of the dwelling where the corrugated steel roof is still present.

4.3. Gas flow velocities at openings

Fig. 17 and Fig. 18 depict the flow velocities of ISD2 for Exp 1 and for B-RISK scenario 1 at the door and window, respectively.

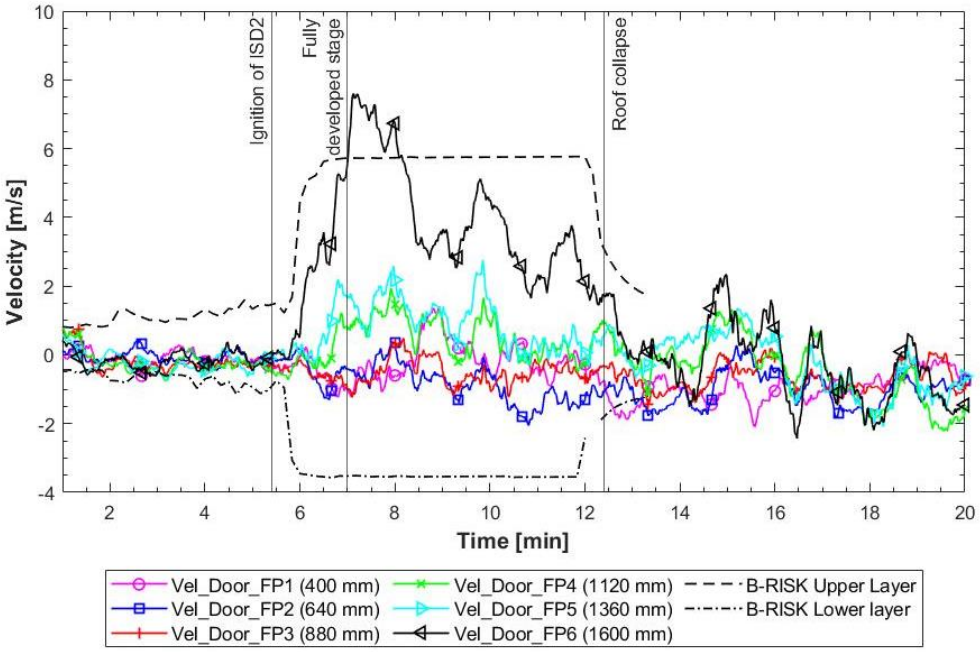

Fig. 17. Flow velocity data at the door of ISD2 for Exp 1 and B-RISK with positive velocity indicating flow out of the dwelling

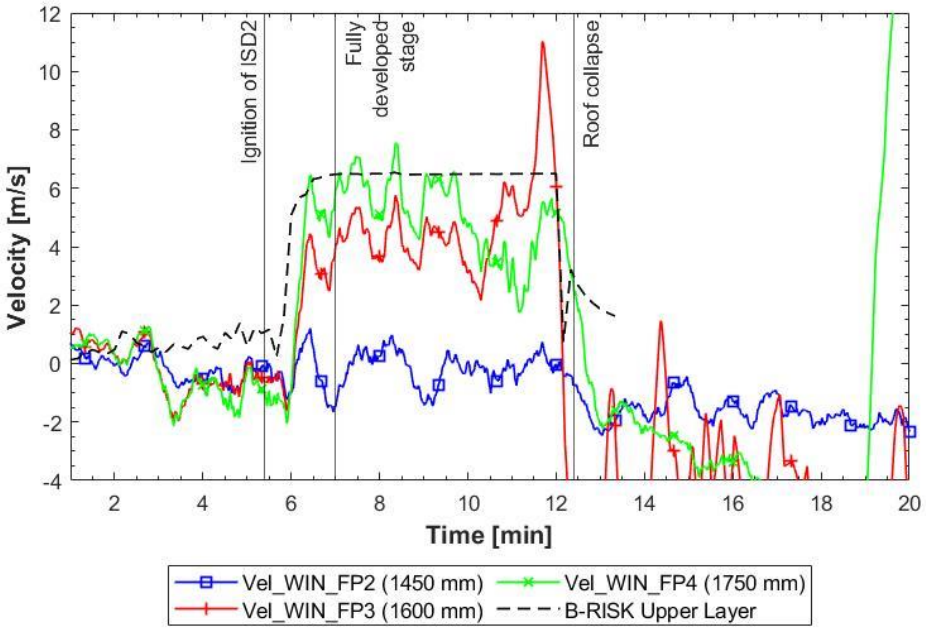

Fig. 18. Flow velocity data at the window of ISD2 for Exp 1 and B-RISK with positive velocity indicating flow out of the dwelling

Considering the experimental door velocities (Fig. 17), the neutral plane is between 900 mm - 1000 mm, which is similar to the 901 mm estimated by B-RISK during the fully developed fire stage. The gas flow velocity out of the window (Fig. 18) is slightly overpredicted by B-RISK. However, there are large discrepancies between the experimental and numerical gas velocities across the door opening (Fig. 17). For the hot gases leaving the enclosure, the discrepancy is likely as a result of the experimental outside pressure fluctuating significantly as the wind speed and direction fluctuates (Fig. 12 a)). For the cold air entering the enclosure, it is clear that B-RISK overestimates the mass flow of air into the enclosure. It is not clear why there is such a large discrepancy between the experimental and numerical results here. Based on a neutral plane height of 900 mm, one can calculate the maximum expected velocity of air entering the enclosure using the following equation [24]:

$$V_{a,max} = \sqrt{\frac{2H_N(\rho_a - \rho_g)g}{\rho_a}} \quad (5)$$

where H_N is the height of the neutral plane (0.9 m in this case), ρ_a is the density of air (assumed to be 1.2 kg/m^3 in this case), ρ_g is the density of the hot gases (assumed to be 0.4 kg/m^3 based on the ideal gas theory) and g is the gravitational acceleration constant. Hence, in this case it is expected that the maximum velocity entering the enclosure should be approximately 3.43

m/s, which seems to correspond well with B-RISK. It does appear that the measurements might be under-quantifying the amount of air entering the dwelling (since air is needed for burning to occur). This could potentially be linked to the leakages allowing air to enter at other places. A plausible explanation could be that air is being sucked in all around the perimeter of the dwelling between the bottom of the dwelling and the floor, since the dwellings were merely placed on the floor. Hence, any eccentricities would have created some gaps for air to enter.

Fig. 19 and Fig. 20 depict the flow velocities at the door and window of ISD2 for Exp 2, respectively.

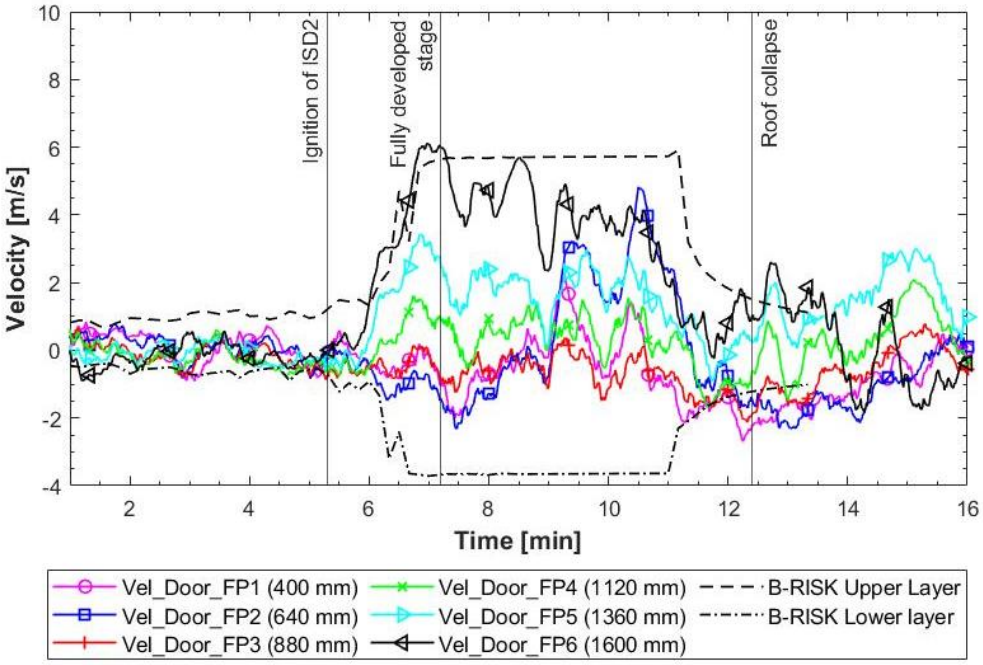

Fig. 19. Flow velocity data at the door of ISD2 for Exp 2 with positive velocity indicating flow out of the dwelling

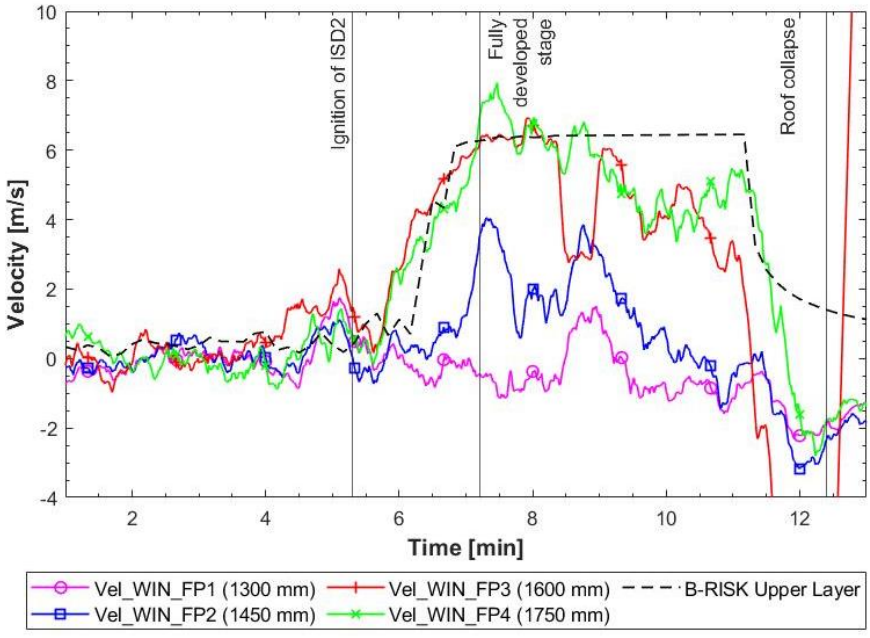

Fig. 20. Flow velocity data at the window of ISD2 for Exp 2 with positive velocity indicating flow out of the dwelling

Considering Fig. 19 and Fig. 20 it is clear that B-RISK captures the trend of the hot gas velocities leaving the dwelling relatively well. Where, similar to above, the deviations can be explained but the fluctuations in wind speed and directions during the experiment (B-RISK cannot account for wind as mentioned before). Similar to Exp 1, B-RISK overpredicts the amount of air entering the enclosure compared to the experimental results. The window velocities (Fig. 20) indicate that the neutral plane of ISD2 for Exp 2 should be at approximately 1300-1350 mm, since the velocities at Vel_WIN_FP1 approximately zero. This is similar to the 1400 mm predicted by B-RISK. However, considering the door velocities (Fig. 19), the neutral plane is approximately 900 mm, which is similar the neutral plane measured during Exp 1. Similar to Exp 1, it is plausible considering the outside pressure at the window (i.e., wind funneling though alley, hot gases pushing from ISD1 to

ISD2, etc.) are different than the outside pressure at the door of ISD2 and this phenomenon (i.e., wind changing the outside pressures) will not be captured in B-RISK as a result of the software's inability to simulate wind.

Fig. 21 and Fig. 22 depict the flow velocities at the door and window of ISD2 for Exp 3, respectively.

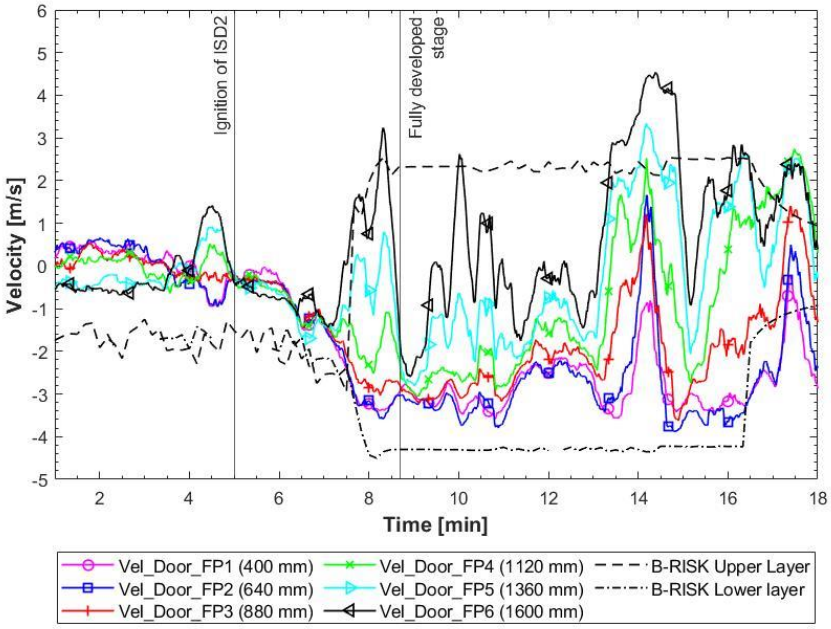

Fig. 21. Flow velocity data at the door of ISD2 for Exp 3 with positive velocity indicating flow out of the dwelling

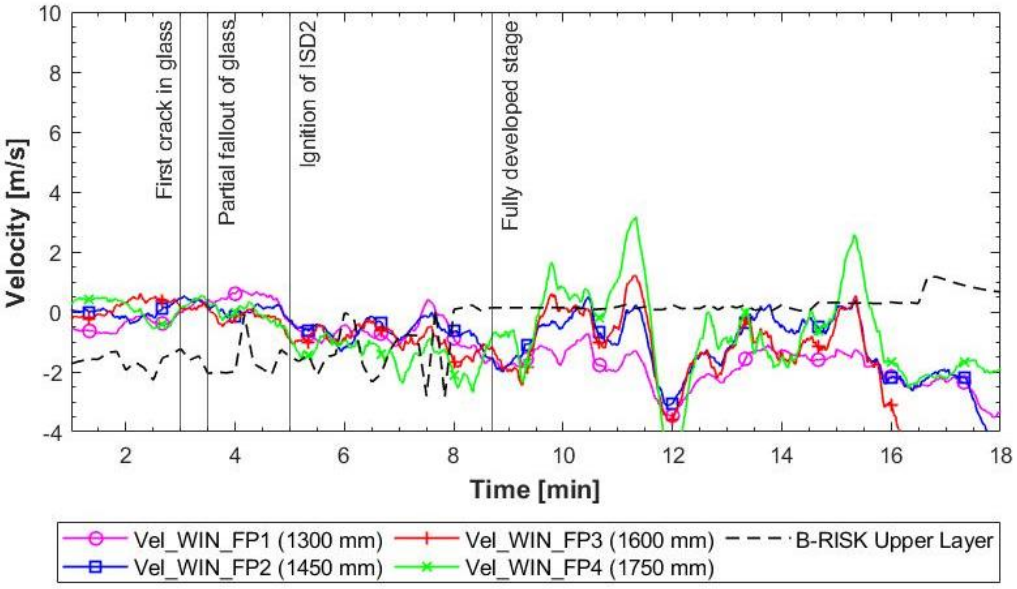

Fig. 22. Flow velocity data at the window of ISD2 for Exp 3

Considering Fig. 21 and Fig. 22 it is clear that the flow out of the door and window was significantly reduced for Exp 3 as a result of the new vent created in the roof opening. It was observed that almost no flames emerged out of the door (Fig. 23 a)) but that approximately all flames were out of the roof vent (Fig. 23 b)). The roof vent also significantly increased the airflow into the dwelling, which is clear by the high inward velocities (Vel_Door_FP1), which increased the amount of oxygen to the cribs and as a result significantly increased the total HRR of the cribs Fig. 13 b). The B-RISK results compare well with the overall trend, however similar to Exp 1 and Exp 2, the software did overpredict the mass flow of air into the enclosure compared to the experiment (however in this case it is closer to the experimental values compared to Exp 1 and Exp 2). Additionally, there are no fluctuations in the B-RISK results, which again is as a result of the software's limitation to simulate wind.

Fig. 23 a) Reduction in flame length emerging out of door for Exp. 3

Fig. 23 b) Flames through roof vent of Exp. 3

4.4. Incident radiation emitted from ISD2

Considering Fig. 14 and Fig. 16, it is clear that adding the roof vent at ceiling level reduced the gas temperatures within ISD2 of Exp 3. Since temperature affects radiation emitted to the power of 4, it is clear that the radiation emitted by the hot gases inside ISD2 for Exp 3 through the door opening will be significantly less compared to ISD 2 for Exp 1 and 2 (since the gas temperature inside ISD2 for Exp 3 is significantly less than Exp 1 and 2). This was evident with the heat fluxes measured at the RW during each experiment, as depicted in Fig. 24.

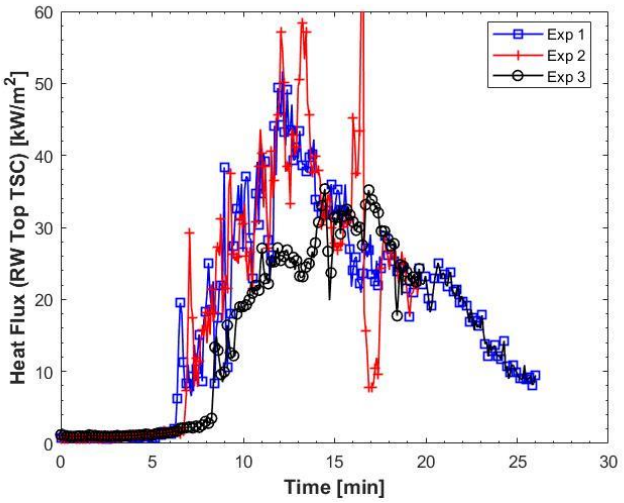

Fig. 24. Heat flux reordered by the top TSC (2 m from ground level) of the RW (2 m for ISD2)

From Fig. 24 it can be seen that the incident heat flux received by the RW peaks at about 50 kW/m^2 for Exp 1. For Exp 2, the incident heat flux received by the RW peaks at about 60 kW/m^2. Although Exp 2 peaks higher than Exp 1, the general heat flux curves between the 2 experiments are relatively similar. For both Exp 1 and Exp 2, a slight peak in heat flux occurs seconds before the fully developed fire stage is reached (i.e., at approximately 6-7 minutes), corresponding to the time where the cardboard lining was engulfed in flames. For Exp 3, the incident heat flux received by the RW peaks just below 35 kW/m^2, with the general heat flux curve being approximately 10-20 kW/m^2 less than Exp 1 and 2. Hence, it can be seen that adding a roof vent (Exp 3) approximately reduced both the average incident heat flux and maximum incident heat flux received at the RW by approximately 25% compared to Exp 1 and Exp 2. Thus, changing the ventilation conditions will affect the radiation emitted and hence will increase or decrease fire spread from one dwelling to another. In addition to the reduction in gas temperature when adding a roof vent, it is clear from experimental observation that the flame lengths ejecting from the door and window significantly reduces, i.e. 2.2 m for Exp 1 (no roof vent) versus 0.4 m for Exp 3 (with roof vent), as listed in Table 3. Hence, this further reduces the risk of fire spread in the direction of flames emitted from the door since the probability for flame impingement onto the neighboring dwellings is reduced. This reduction in flame length is strongly linked to the movement of the neutral plane. Increasing the ventilation increases the height of the neutral plane, which results in lower gas

flow velocities exiting the dwelling. However, now a large fire plume ejects from the roof (see Fig. 23 b)) of ISD2 for Exp 3, which now radiates in all directions. This means that there are potential new fire spread pathways in multiple directions which could auto-ignite items if close enough.

The predictive capabilities within B-RISK can be used to indirectly estimate how much radiation is emitted by this fire plume ejecting from the roof. Fig. 25 depicts the B-RISK predicted incident radiation that falls onto the inner wall of the dwelling for ISD2. This can also be seen as the radiation intensity at the door of the dwelling as a result of the hot gases. In other words, if one assumes that the door opening acts as a radiant panel (hot gases being the source of heat), the radiation depicted in Fig. 25 is the radiation at the door opening (excluding the external flames). Hence, we can now calculate the radiation component of the hot gases at two meters away from the door (where the TSC was located in the experiment) using a configuration factor between the door opening and the TSC location at the RW (located 2 m away from ISD2 at a height of 2 m from the ground, in front of the door).

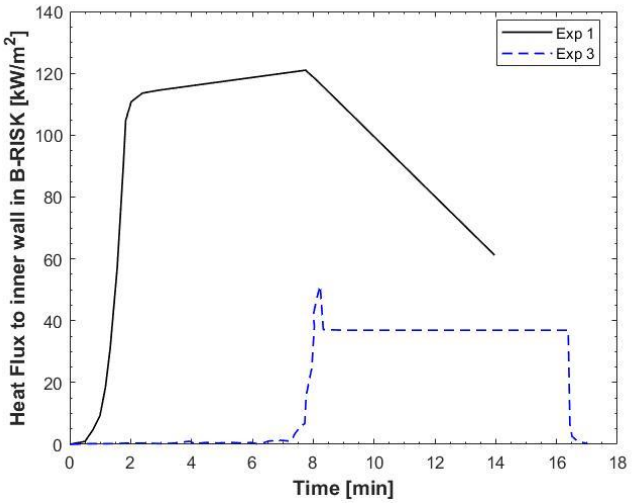

Fig. 25. Incident radiation to inner wall in B-RISK, which can be seen as the radiation intensity at the door.

The configuration factor (otherwise known as a view factor) for this scenario is equal to 0.32 (configuration factor was calculated as done in ref. [12]), implying that the maximum radiation received by the TSC at 2 m away from the door as a result of the hot gases in ISD2 was 38.4 kW/m^2 for Exp 1 and 15.0 kW/m^2 for Exp 3, based on the B-RISK predictions. Comparing these values to the maximum heat fluxes depicted in Fig. 24 of 50 kW/m^2 for Exp 1 and 35 kW/m^2 for Exp 3, one can estimate the radiation component of the flame ejecting from the door of Exp 1 and for the flame ejecting from the roof vent in Exp 3 (assuming the radiation component of the steel sheets are negligible at 2 m – which is what was found in ref. [12]). For Exp 1, the radiation received at 2 m away from the door as a result of the door flame is thus 50 kW/m^2 (measured value) minus 38.4 kW/m^2 (gas component as predicted by B-RISK), which gives 11.6 kW/m^2. For Exp 3, the radiation received at 2 m away from the door as a result of the flame emerging from the roof (no flames from the door in this case, hence one can safely assume the radiation from the door flame is 0 kW/m^2) is thus 35 kW/m^2 (measured value) minus 15.0 kW/m^2 (gas component as predicted by B-RISK), which gives 20.0 kW/m^2. This implies that although adding the roof vent reduced the radiation measured in front of the door opening, compared to Exp 1, it increases the radiation emitted in all other directions by approximately 20 kW/m^2 at 2 m away from the edge of the flame emerging from the roof, which is sufficient to ignite most common combustible materials, assuming a piloted source is present. In a dense settlement adjacent homes within 1-2m often have thin plastic linings, newspaper draft stoppers, hanging washing or other materials at roof level which may ignite readily due to their low thermal inertia and ignition temperatures. Furthermore, large IS conflagrations typically occur during high wind conditions, which would cause flames emerging from roofs to tilt towards adjacent dwellings.

Given the diversion of the external flaming from horizontal openings to the roof opening, it is much less likely that areas of high radiation are spatially incident with a flame to cause piloted ignition. Therefore, the scenario becomes a trade-off between piloted ignition adjacent to openings, and auto-ignition in other areas. Auto-ignition is a complex phenomenon and there are few, if any, comprehensive studies which directly compare auto-ignition heat fluxes or temperatures with corresponding piloted ignition properties for multiple materials. A recent summary of previous studies concluded that critical heat fluxes of wooden materials range from 10-13 kW/m^2 under piloted conditions, but are significantly higher at 25-33 kW/m^2 under auto-ignition conditions [25]. Another study of wooden materials found that under medium level heat fluxes, where auto-ignition could occur, it may still take over 200 seconds longer than under piloted conditions at the same flux [26].

4.5. Radiation to floor level of ISD2

During each experiment, one TSC was placed on each crib in ISD2 to measure the radiation to the cribs as a result of (i) the hot gases before the cardboard ignited and (ii) the radiation to the cribs after the cardboard ignited. The crib TSCs were 700 mm from the floor (i.e., the crib plus scale plus scale protection height). Fig. 26 depicts the incident radiation to the wood

cribs for Exp 1, 2 and 3. The TSC placed on the front crib of ISD2 in Exp 1 broke and gave invalid readings. Thus, only the back crib incident heat flux is depicted in Fig. 26 for Exp 1. It should be noted that the extension cable of the TSCs are only rated to 200°C, although also protected in ceramic blanket, once flashover commences the cables inside the dwelling will still melt and the data afterwards should be ignored in this case. Fig. 27 depicts the incident radiation to floor lever for Exp 1, 2 and 3 predicted by B-RISK.

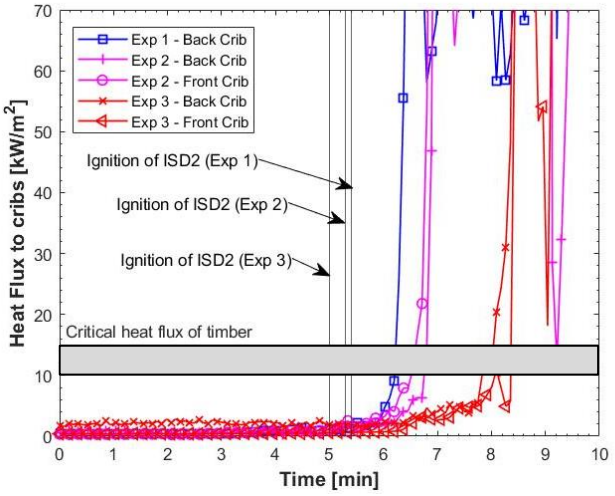

Fig. 26. Incident heat flux received by cribs (experimental results)

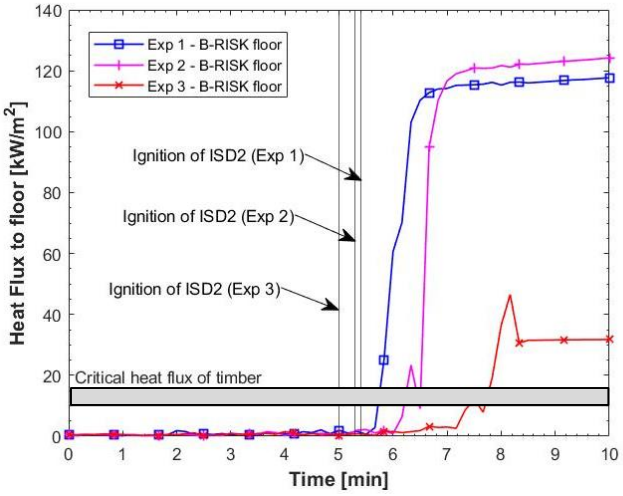

Fig. 27. Incident heat flux received by cribs (numerical results)

Fig. 26 shows that the heat flux to the cribs before ignition is negligible (i.e., significantly lower than the critical heat flux of the crib timber pieces, which is around 10-15 kW/m^2 [27,28]). However, it is clear that as soon as the fire spread rate across the surface of cardboard lining starts to accelerate, the energy release, and subsequently the heat fluxes emitted to crib level, is significant (i.e., > 100 kW/m^2) and is more than enough to induce flashover. By considering the time from ignition of ISD2 to the onset of flashover of ISD2 (both looking at Fig. 26 and Fig. 27), it is clear that the more ventilation present at ceiling level, the longer the time to the onset to flashover, i.e. since more openings allow the hot gases to escape from the enclosure quicker.

5. PARAMETRIC STUDY

Comparing the numerical results above to the experimental results, it is clear that B-RISK does capture the overall behavior of the ISDs studied in this work, at most measurement locations (e.g., the upper layer temperature and velocities of hot gases leaving the enclosure), well. There are however certain measurements where the experimental and numerical results do not compare well, e.g. the mass flow of air entering the enclosure. The authors are, however, uncertain why there are such discrepancies and are uncertain whether the problem is numerical or experimental, although it is possibility related to the permeable nature of the dwellings and the interactions with wind. However, with the exception of the inflow velocities, B-RISK can be used for a parametric investigation with a fair level of confidence. In this section, the following ventilation parameters are further investigated: a) the window aspect ratio (keeping the area of the opening the same and the window soffit at 1.85 m), b) the window opening size (keeping the aspect ratios the same and the window soffit at 1.85 m) and c) the sill height of the window (keeping both the opening size and aspect ratio the same). The effects of leakages and ventilation conditions on IS fire spread are not well understood and how these conditions should be incorporate in statistical fire spread models [9,10] for IS dwellings are unclear. Hence, if simple tools, like B-RISK, can be used to determine these effects, it would be beneficial for the further development of these statistical models.

For all the simulations that follow, the geometry of the ISD of Exp 1 is used, with the same inputs as described in Section 3 above. However, in this case a simplified HRR curve was assigned to each crib, as depicted in Fig. 28, as opposed to the measured HRR. The heat release rate of the crib was determined using Equations 2-4 above and it was found that the crib is porosity-controlled.

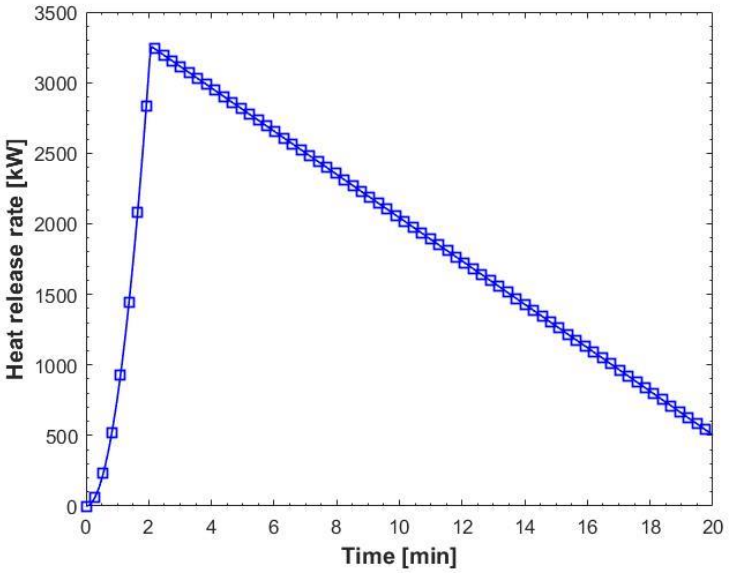

Fig. 28. Heat release rate input used per crib in B-RISK

5.1. Window aspect ratio

In this section, the effect of the window aspect ratio on the maximum upper layer temperature, gas flow velocities and the time to flashover are investigated, while keeping the window area the same. Table 4 summarizes the numerical inputs and outputs of this parametric study. In all cases, the window soffit height was kept at 1.85 m as per experiments.

Table 4: Summary of the numerical inputs and outputs for the window aspect ratio parametric study.

Scenario	Window aspect ratio (H/W)	Window area (m^2)	Maximum upper layer temperature (°C)	Maximum door velocity (m/s)	Time to flashover (s)
Baseline (BL)	0.71	0.51	947	5.79	66
Scenario 2 (S2)	1.25	0.51	942	5.8	65
Scenario 3 (S3)	1.96	0.51	936	5.82	65
Scenario 4 (S4)	2.82	0.51	934	5.88	65
Scenario 5 (S5)	3.84	0.51	935	5.97	65

The results listed in Table 4 clearly shows that the window aspect ratio has a negligible effect on the maximum upper layer temperature, gas flow velocities and the time to flashover. The parameter most affected is the gas flow velocities. It appears that as the aspect ratio increases, the maximum gas flow velocity at the door increase, implying that the horizontal flame length will increase, which increases the probability of flame impingement onto the adjacent dwelling.

5.2. Window opening size

In this section, the effect of the window opening size on the maximum upper layer temperature, gas flow velocities and the time to flashover is investigated, while keeping the window aspect ratio the same. Table 5 summarizes the numerical inputs and outputs of this parametric study. In all cases, the window soffit height was kept at 1.85 m as per experiments.

Table 5: Summary of the numerical inputs and outputs for the window area size parametric study.

Scenario	Window area (m^2)	Ventilation factor ($m^{1.5}$)	Maximum upper layer temperature (°C)	Maximum door velocity (m/s)	Time to flashover (s)
Baseline (BL)	0.51	0.4	947	5.79	66
Scenario 2 (S2)	0.9	0.81	966	5.67	68
Scenario 3 (S3)	1.41	1.41	979	5.66	71

Scenario 4 (S4)	2.03	2.22	985	5.77	74
Scenario 5 (S5)	2.76	3.27	928	5.73	79

The results depicted in Table 5 indicate that as the opening size (and as a result the opening factor) increases, the maximum upper layer gas temperature increases. This is true for Scenario 1 (BL scenario) to Scenario 4, however once the ventilation controlled HRR surpasses the maximum HRR of the fuel (6.4MW) the maximum gas temperature starts to decrease as the opening size (and as a result the opening factor) increases. One can easily determine the critical ventilation factor at which the fully developed fire will no longer be ventilation controlled using Equation 1, where $\dot{m}$ is set equal to the maximum HRR of the fuel divided by the heat of combustion of the fuel:

$$\frac{6400}{17000} = 0.12A_o\sqrt{H_o} \quad (6)$$

this then gives a ventilation factor ($A_o\sqrt{H_o}$) of 3.14 $m^{1.5}$ (this point is referred to as the critical ventilation limit for the rest of this section). Hence, for Scenario 4 we can clearly see that the fire is still ventilation controlled during the fully developed fire stage (i.e., 2.22 < 3.14 $m^{1.5}$) and thus the gas temperature increased, but Scenario 5 is now fuel controlled during the fully developed fire stage (i.e., 3.27 > 3.14 $m^{1.5}$) and thus the gas temperature started to decrease. This implies that adding or removing openings or changing their size will only have the benefit of decreasing the gas temperatures if it results in a real ventilation factor sufficiently above or below that of the critical ventilation limit. Assuming the critical ventilation limit as a baseline, it is noteworthy that a small increase in ventilation area from this critical value will result in a greater reduction in gas temperature than an equal decrease in area. However, this must be treated as a trade-off with the fact that lower opening areas will result in lower configuration factors between the openings and receiving dwellings. Thus, if an ISD has a high fuel load density [3,29] or contains naturally fast-burning fuels, one must be careful to ensure that a change to the openings does not increase the fire spread risk by moving the ventilation factor closer to the critical value. However, in a scenario where the ISD has a low fuel load or slow burning materials, the critical ventilation limit will be a lower value and so there is a much higher probability that adding openings will consistently increase the ventilation factor above the critical value, thus decreasing temperatures. Additionally, if the receiving (target) dwelling has more openings it increases the probability of the dwelling being ignited, because there are more spaces for flames to impinge on combustibles.

The B-RISK parametric results in Table 5, further highlights that as the ventilation factor increases, the time to flashover increases. This is well known within the fire community and can be described in terms of the following equation [30]:

$$\dot{Q}_{FO} = 610\left(h_k A_T A_o\sqrt{H_o}\right)^{1/2} \quad (7)$$

where $\dot{Q}_{FO}$ is the minimum HRR needed for flashover to occur, h_k is the effective heat transfer coefficient (h_k for thermally thin boundaries, such as informal settlement boundaries, has been investigated in depth by Beshir et al. [31]) and A_T is the total enclosing area of the compartment. Hence, from Equation 7, it is clear that as the ventilation factor increases, the minimum HRR needed for flashover increases, implying that the time to reach that HRR will increase.

5.3. Window soffit height

In this section, the effect of the window soffit height on the maximum upper layer temperature, gas flow velocities and the time to flashover is investigated, while keeping the window aspect ratio and area the same. Table 6 summarizes the numerical inputs and outputs of this parametric study.

Table 6: Summary of the numerical inputs and outputs for the window soffit height parametric study.

Scenario	Window soffit height (m^2)	Maximum upper layer temperature (°C)	Maximum door velocity (m/s)	Time to flashover (s)
Baseline (BL)	1.85	947	5.79	66
Scenario 2 (S2)	1.65	938	5.81	65
Scenario 3 (S3)	1.45	927	5.84	64
Scenario 4 (S4)	1.25	918	5.95	64
Scenario 5 (S5)	1.05	918	6.10	64

Comparing Tables 4-6 it is clear that the window soffit height has the largest effect on both the maximum gas temperature reached and the maximum door gas flow velocities reached. Considering Fig. 29, it becomes clear that as the soffit height increases, the height of the neutral plane height increases. This then leads to a decrease in the gas flow velocities at the door (meaning shorter horizontal flames emerging from the door), which allows for less hot gases to leave the enclosure (i.e., less heat loss by convection) allowing for higher gas temperatures (meaning higher radiation being emitted).

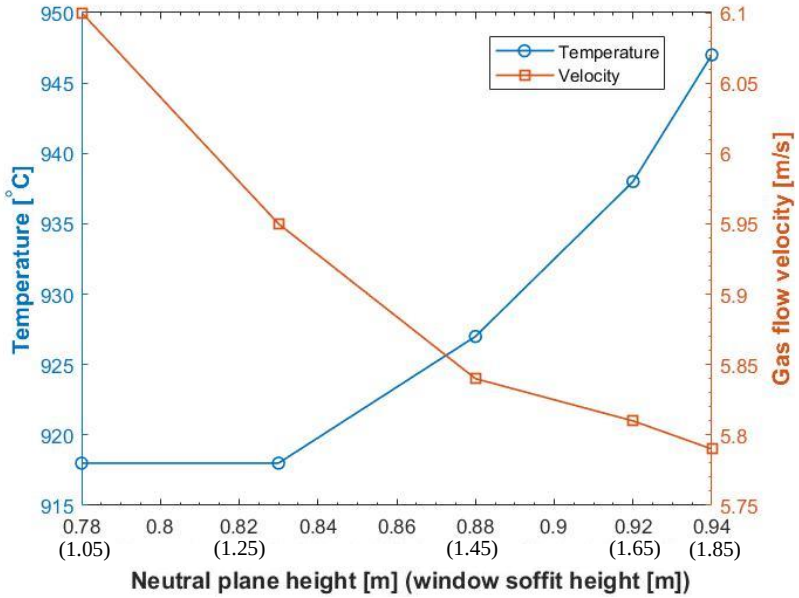

Fig. 29. The effect of the window soffit height on a) the neutral plane height, b) the gas temperature and c) the gas flow velocities at the door

6. CONCLUSION

This paper investigated the effects of leakages and ventilation conditions on the fire dynamics in informal settlements, with a key interest on the fire spread behavior. This work will be beneficial for the development of statistical fire spread models that can approximately predict fire spread through informal settlements. Ignition and time-temperature, or time-heat flux, sub-models of individual homes can be defined in more detail based on the results obtained (i.e., since this work showed that simple two-zone model software can be used to generate these sub-models for statistical fire spread models, as opposed to complex computational fluid dynamics software)

In this work, 3 full-scale informal settlement experiments were conducted. Each experiment consisted of two dwellings. The differences between the three experiments were kept to a minimum, with only one leakage or ventilation condition being changed from experiment to experiment. B-RISK (a two-zone fire model software) was used to simulate the three experiments conducted in this work. The B-RISK results showed relatively good correlation to the experimental results, thus the software was further utilized by conducting a parametric study on the following ventilation parameters: a) the window aspect ratio (keeping the area of the opening the same), b) the opening size (keeping the aspect ratios the same) and c) the sill height of the window (keeping both the opening size and aspect ratio the same).

- The data showed that having leakages (i.e., open flutes), ISD2 experiences less heat build-up which means that once the cardboard lining ignites, the spread rate across the surface is reduced as a result of a reduction in the preheating of the cardboard. Additionally, leakages cause the peak HRR inside the dwelling to slightly increase, as a result of the increase in the ventilation factor. Leakages did, however, not significantly influence the maximum flame lengths ejecting from the door or the heat fluxes emitted from the openings. This is beneficial for future computational modelling as it is not easy to account for the presence of the commonly found small openings in people's homes.
- It was observed that adding a roof vent significantly reduced the flame lengths from the door opening and also reduced the heat fluxes emitted from the door opening, reducing spread in the direction of side openings. However, the data further indicated that a roof vent significantly increased the peak HRR, by around 40%, since it raises the neutral plane significantly, allowing more oxygen to enter the dwelling and hence changing the burning regime from ventilation-controlled to fuel-controlled. The plume emitted radiation in all directions with calculated fluxes in the order of 20 kW/m^2 at 2 m, meaning that fire can spread radially (possibly igniting combustible roof linings such as plastic sheets) and not only in the directions defined by side openings.
- The parametric study showed that changing the opening aspect ratios had virtually no effect of the enclosure fire dynamics. Assuming ISDs have a high fuel load density, the parametric studied showed that more openings increase the probability of a dwelling igniting its neighboring dwelling, and also increases the probability of the dwelling being ignited, but it does however delay the time to flashover once ignited.

7. ACKNOWLEDGEMENTS

The authors would like to gratefully acknowledge Breede Valley Fire Department and two undergraduate students, Monique Scheepers and Kyle Stebbing, from Stellenbosch University for their contribution and assistance towards helping the authors

successfully complete the experiments. This work is financially supported by IRIS-Fire GCRF project from the UK (Engineering and Physical Sciences Research Council Grant no.: EP/P029582/1), the Lloyd's Register Foundation under the "Fire Engineering Education for Africa" project (Grant GA 100093).

8. REFERENCES

[1] City of Cape Town, Increase in residential fires and related fatalities are cause for concern, (2019).

[2] UN-Habitat, Slum Almanac 2015/2016: Tackling Improvement in the Lives of Slum Dwellers, Nairobi, 2016.

[3] R. Walls, G. Olivier, R. Eksteen, Informal settlement fires in South Africa: Fire engineering overview and full-scale tests on "shacks," Fire Safety Journal. 91 (2017) 997–1006. https://doi.org/10.1016/j.firesaf.2017.03.061.

[4] A. Cicione, M. Beshir, R.S. Walls, D. Rush, Full-Scale Informal Settlement Dwelling Fire Experiments and Development of Numerical Models, Fire Technology Journal. (2019). https://doi.org/10.1007/s10694-019-00894-w.

[5] Y. Wang, L. Gibson, M. Beshir, D. Rush, Determination of Critical Separation Distance Between Dwellings in Informal Settlements Fire, Fire Technology. (2021). https://doi.org/10.1007/s10694-020-01075-w.

[6] A. Cicione, R.S. Walls, C. Kahanji, Experimental study of fire spread between multiple full scale informal settlement dwellings, Fire Safety Journal. 105 (2019) 19–27. https://doi.org/10.1016/j.firesaf.2019.02.001.

[7] M. Beshir, K. Omar, F.R. Centeno, S. Stevens, L. Gibson, D. Rush, Experimental and numerical study for the effect of horizontal openings on the external plume and potential fire spread in informal settlements, Applied Sciences (Switzerland). 11 (2021). https://doi.org/10.3390/app11052380.

[8] M. Beshir, A. Cicione, Y. Wang, S. Welch, D. Rush, Re-visiting NIST Reduced / Full-Scale Enclosures (R / FSE) Experiments (2007-2008), in: Interflam Proceedings, 2019: pp. 2095–2107.

[9] A. Cicione, C. Wade, M. Spearpoint, L. Gibson, R.S. Walls, D. Rush, A preliminary investigation to develop a semi-probabilistic model of informal settlement fire spread using B-RISK, Fire Safety Journal. 120 (2021).

[10] A. Cicione, L. Gibson, C. Wade, M. Spearpoint, R. Walls, D. Rush, Towards the development of a probabilistic approach to informal settlement fire spread using ignition modelling and spatial metrics, Fire. 3 (2020) 1–26. https://doi.org/10.3390/fire3040067.

[11] Y. Wang, M. Beshir, A. Cicione, R. Hadden, M. Krajcovic, D. Rush, A full-scale experimental study on single dwelling burning behavior of informal settlement, Fire Safety Journal. (2020) 103076. https://doi.org/10.1016/j.firesaf.2020.103076.

[12] A. Cicione, R. Walls, Z. Sander, N. Flores Quiroz, V. Narayanan, S. Stevens, D. Rush, The effect of separation distance between informal dwellings on fire spread rates based on experimental data and analytical equations, Fire Technology. (2020).

[13] A. Cicione, M. Beshir, R.S. Walls, D. Rush, Full-Scale Informal Settlement Dwelling Fire Experiments and Development of Numerical Models, Springer US, 2019. https://doi.org/10.1007/s10694-019-00894-w.

[14] N. de Koker, R.S. Walls, A. Cicione, Z.R. Sander, S. Löffel, J.J. Claasen, S.J. Fourie, L. Croukamp, D. Rush, 20 Dwelling Large-Scale Experiment of Fire Spread in Informal Settlements, Fire Technology. 56 (2020). https://doi.org/10.1007/s10694-019-00945-2.

[15] A. Cicione, R.S. Walls, C. Kahanji, Experimental study of fire spread between multiple full scale informal settlement dwellings, Fire Safety Journal. 105 (2019) 19–27. https://doi.org/10.1016/j.firesaf.2019.02.001.

[16] M. Beshir, Y. Wang, L. Gibson, S. Welch, D. Rush, A Computational Study on the Effect of Horizontal Openings on Fire Dynamics within Informal Dwellings, Proceedings of the Ninth International Seminar on Fire and Explosion Hazards (ISFEH9. (2019) 512–523. https://doi.org/10.18720/spbpu/2/k19-122.

[17] CEN, Eurocode 1: Actions on structures -Part 1: General actions - Actions on structures exposed to fire, CEN, 2002.

[18] M.A. Delichatsios, Fire Growth Rates in Wood Cribs, Combustion and Flame. 27 (1976) 267.

[19] V. Babrauskas, Heat release rates, in: M.J. Hurley et. al (Ed.), SFPE Handbook of Fire Protection Engineering, 5th ed., Springer, 2016: p. 829. https://doi.org/10.1007/978-1-4939-2565-0.

[20] C. Wade, G. Baker, K. Frank, R. Harrison, M. Spearpoint, BRANZ Study report SR364 B-RISK 2016 user guide and technical manual, 2016.

[21] A. Tewarson, Generation of Heat and Chemical Compounds in Fires, in: P.J. DiNenno (Ed.), SFPE Handbook of Fire Protection Engineering, 3rd ed., 2016: pp. 277–324. https://doi.org/10.1007/978-1-4939-2565-0_9.

[22] B.J. McCaffrey, J.G. Quintiere, M.F. Harkleroad, Estimating room temperatures and the likelihood of flashover using fire test data correlations, Fire Technology. 17 (1981) 98–119. https://doi.org/10.1007/BF02479583.

[23] M.A. Delichatsios, Fire Growth Rates in Wood Cribs, Combustion and Flame. 27 (1976) 267.

[24] B. Karlsson, J.G. Quintiere, Enclosure fire dynamics, CRC Press, London, New York, Washington D.C., 2000. https://doi.org/10.1016/S0379-7112(01)00031-5.

[25] A.I. Bartlett, R.M. Hadden, L.A. Bisby, A Review of Factors Affecting the Burning Behaviour of Wood for Application to Tall Timber Construction, Fire Technology. 55 (2019) 1–49. https://doi.org/10.1007/s10694-018-0787-y.

[26] W. Jaskolkowski, P. Ogrodnik, A. Lukaszek-Chmielewska, The study of time to ignition of woods external heat flux by piloted ignition and autoignition, Annals of Warsaw University of Life Sciences - SGGW. Forestry and Wood Technology. 86 (2014) 133–137.

[27] Y. Wang, C. Bertrand, M. Beshir, C. Kahanji, R. Walls, D. Rush, Developing an experimental database of burning characteristics of combustible informal settlement dwelling materials, Fire Safety Journal. (2019). https://doi.org/https://doi.org/10.1016/j.firesaf.2019.102938.

[28] Y. Wang, D. Rush, Cone calorimeter tests of combustible materials found in informal settlements, [dataset], (2019).

[29] A. Cicione, R.S. Walls, C. Kahanji, Experimental study of fire spread between multiple full scale informal settlement dwellings, Fire Safety Journal. (2019). https://doi.org/10.1016/j.firesaf.2019.02.001.

[30] D. Drysdale, An introduction to fire dynamics, 3rd ed., Wiley, Chichester, 2011.

[31] M. Beshir, M. Mohamed, S. Welch, D. Rush, Modelling the Effects of Boundary Walls on the Fire Dynamics of Informal Settlement Dwellings, Fire Technology. (2021). https://doi.org/10.1007/s10694-020-01086-7.

An experimental and numerical study on the effects of leakages and ventilation conditions on informal settlement fire dynamics

ABSTRACT

The one billion people that currently reside in informal settlements are exposed to a high and daily risk of large conflagrations. With the number of informal settlement dwellers expected to increase in the years to come, more systematic work is needed to better understand these fires. Over the past 3-4 years, researchers have explicitly started investigating informal settlement fire dynamics, by conducting full-scale experiments and numerical modelling research. It is with this background that this paper seeks to investigate the effects of leakages and ventilation conditions on informal settlement fire dynamics. Three full-scale informal settlement dwelling experiments were conducted in this work. The experiments were kept identical with only a small change to a ventilation or leakage condition from experiment to experiment. During each experiment the heat release rates, heat fluxes, temperature and flow data were recorded and are given in this paper. B-RISK's (a two-zone model software) predictive capabilities are then benchmarked against the full-scale experiments. B-RISK is then used to conduct a parametric study to further investigate the effects of leakages and ventilation on informal settlement dwelling fire dynamics. It was found that the ventilation conditions can significantly affect the radiation emitted from an informal settlement dwelling, and as a result increase or decrease the probability of fire spread to neighboring dwellings.

KEYWORDS: informal settlements, fire spread, enclosure fire dynamics, two-zone modelling.

1. INTRODUCTION

Despite the increase in informal settlement fire research and efforts for awareness, the number of informal settlement fire incidents are still increasing annually (e.g., in December 2019, Cape Town alone had 268 informal settlement fires, which is 23% more that in December 2018 [1][~~1~~]). Currently, there are approximately 1 billion people residing in informal settlements worldwide, and this number is expected to rapidly increase in the next 20-30 years [2][~~2~~]. With the number of informal settlement fires increasing annually, and since the number of informal settlement dwellers are expected to increase, there is a great need to better understand the factors that contribute towards large conflagrations in informal settlements on a fundamental level. Fig. 1 and Fig. 2 visually show typical informal settlement dwellings (ISDs) and an informal settlement, respectively, found in South Africa.

Fig. 1. Example of typical ISDs

Fig. 2. Informal settlement in Cape Town, South Africa

In the past few years, researchers have developed a preliminary understanding of informal settlement fire dynamics by applying early–stage Fire Dynamics Simulator (FDS) simulations to scenarios of interest, and by conducted preliminary fire spread experimental investigations. The first ISD experiments, were conducted by Walls et al. [3][~~3~~], where the study found that these makeshift dwellings behave similar to what one would expect of formal enclosures, i.e. informal dwellings experience ignition, a growth phase, flashover, a ventilation-controlled fully developed fire stage and a decay period (which is typically curtailed due to structural collapse for informal dwellings). Cicione et al. [4][~~4~~] continued the investigation of the informal settlement fire problem by conducting a series of full-scale experiments. Their experiments specifically focused on the effect of cladding materials on the internal fire dynamics and fire spread rates for informal settlements. The study further applied FDS to specific scenarios of the experiments conducted and from the simulation results it was found that dwellings spaced at approximately 3 m are not susceptible to fire spread (in 'still' wind conditions). This finding is similar to that found by Wang et al. [5][~~5~~] and Cicione et al. [6][~~6~~] where they estimated the critical separation distance between dwellings for fire spread not to occur, under still wind conditions, to be approximately 3-4 m. Beshir et al. [7][~~7~~] conducted a numerical investigation (using FDS) on the effect of horizontal roof openings on the internal fire dynamics of ISDs as well as on the heat fluxes emitted by these dwellings. They found that dwellings with a horizontal roof vent had a slower time to flashover

and emitted lower heat fluxes to its surroundings. Beshir et al. [8]~~[8]~~ continued the numerical investigation of vents (using FDS), with the focus shifted to the effect of vertical opening positions with respect to a door opening. It was found that the position of a vertical opening with respect to a door opening also has an effect on the heat fluxes emitted. Cicione et al. [9,10]~~[9,10]~~, looked at the possibility of simulating informal settlement fire spread using a semi-probabilistic approach. Although, the method showed real potential, a number of variables are still unknown that are needed to further develop the proposed method. One of these unknown variables is the effect of ventilation conditions on the radiation emitted by an ISD, which is investigated in the paper. Wang et al. [11]~~[11]~~ looked at the effect of ventilation conditions on ISD fire dynamics (dwelling scale), in laboratory conditions. Research relating to ISD fires is relatively immature and therefore there is a paucity of specific literature called upon above.

The research mentioned above has provided a basis for informal settlement fire dynamics, but there is still a significant need to answer specific questions on a more fundamental level. It is with this in mind that this paper seeks to answer a very specific question: How do leakages and ventilation conditions effect informal settlement (both on a settlement and dwelling scale) fire dynamics?

2. EXPERIMENTAL SET-UP

In December 2019, a series of full-scale informal settlement fire experiments were conducted at Breede Valley Fire Department, in Worcester, South Africa. In this work, only 3 of the 9 experiments are discussed. As mentioned above, the focus of this paper is on the effect of leakages and ventilation conditions on ISD fire dynamics, hence only the experiments contributing towards better understanding these effects are included here. From the other six experiments, t~~T~~wo experiments focused on the effect of separation distance on fire spread can be found in Cicione et al. [12]~~[12]~~;. t~~T~~hree experiments investigated the effect of different lining materials on the fire spread rates and internal fire dynamic; ands~~.~~ o~~O~~ne experiment was a double storey informal settlement dwelling, another experiment looked at the effect of internal divisions on the ISD fire dynamics. The general experimental setup of the 3 experiments considered in this work is identical, as depicted in Fig. 3. All experiments consisted of two dwellings denoted ISD1 (left dwelling in Fig. 3) and ISD2 (right dwelling in Fig. 3).

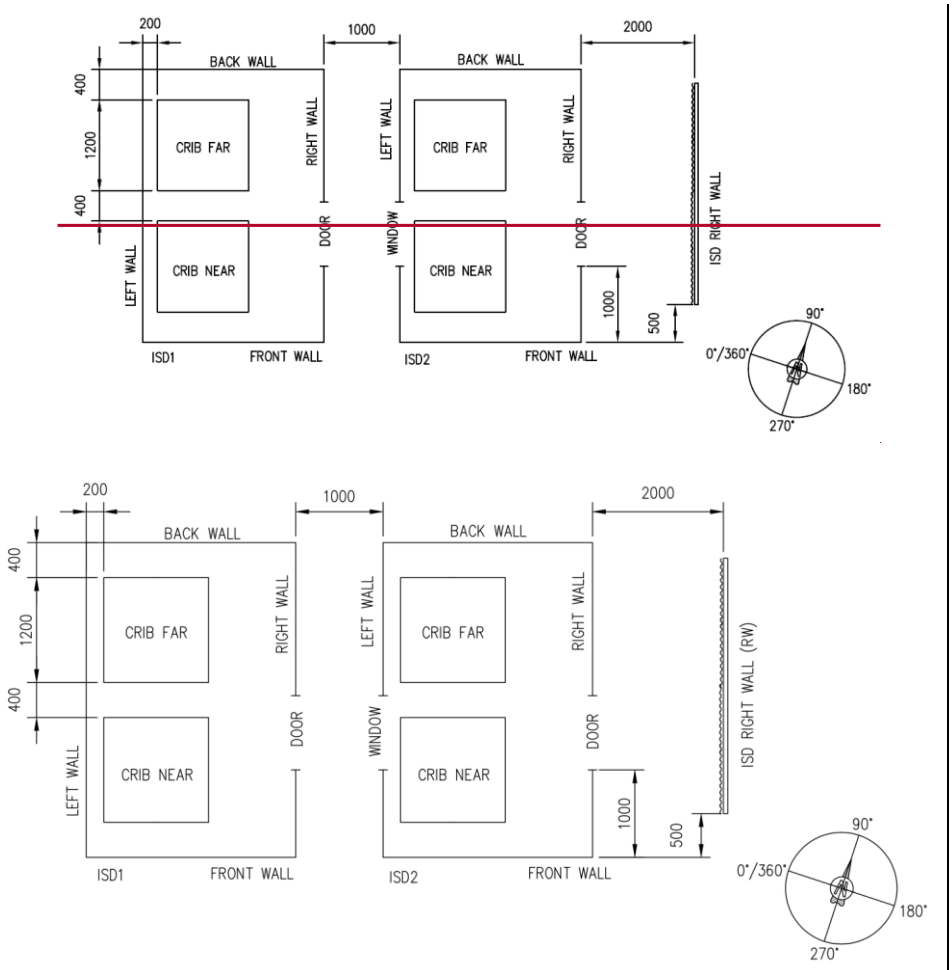

Fig. 3. Experimental setup, with ISD1 being the dwelling of origin, the fire spreading to ISD2. Units are in mm.

In all experiments, the dwelling on the left in Fig. 3 was the dwelling of fire origin and is denoted as ISD1 for the remainder of the paper. The fire was then left to spread from ISD1 to the target dwelling, the dwelling on the right of Fig. 3, and is denoted as ISD2. All experiments had the exact same general setup, but for each experiment ISD2 had a change in its ventilation- or leakage condition. ISD1 was ignited by igniting 8 small bags, filled with a 400 mm × 400 mm of kerosene dipped hessian, with one bag placed at each of the bottom 4 corners of each crib (similar to what was done in [11,12]~~[11,12]~~). A lone standing wall was setup, upon which heat fluxes were measured, and is referred to as ISD Right Wall (denoted as RW), as depicted in Fig. 3.

2.1. Design of dwellings

All dwellings used in these experiments had a floor area identical to that of the ISO 9705 room (3.6 m×2.4 m), and were 2.3 m in height, similar to those used in previous ISD research [3,11,13–15]~~[3,11,13–15]~~. Since informal dwelling construction methods and materials have been discussed in detail by numerous researchers, it is not included here. However, should the reader require more information regarding informal dwelling construction materials etc. the reader should refer to refs. [3,11,13–15]~~[3,11,13,14,16]~~. For all experiments, ISD1 was clad with IBR (inverted box rib) sheeting that was fixed to a steel frame. Steel sheeting, which is typically galvanized, is one of the most common cladding materials used in informal

settlements [3,14][~~3,16~~]. In order to reproduce a consistent fire scenario in ISD1, such that all 3 experiments had a similar fire in ISD1, the dwelling only had one opening, a door with an internal dimension of 2.05 m (height) × 0.85 m (width), no cardboard lining (as one would typically find in an ISD [3,11,13–15][~~3,11,13,14,16~~]) and all openings created by the flutes of the IBR sheets (38 mm flute height) were closed with ceramic blanket (in reality the openings created by flutes are often left open, stopped with clay or even combustible materials such as newspaper). For all experiments, ISD2 was clad with corrugated steel sheets, that were fixed to SA pine timber frames (50 mm × 50 mm) with an approximate density of 450 kg/m^3, and were lined with cardboard mimicking the highly flammable lining and contents present in many real ISDs [6][~~6~~]. ISD2 had two openings: (1) a window opening with an internal dimension of 0.6 m (height) × 0.85 m (width), with the window ~~-~~sill placed 1.25 m from ground level, and (2) a door opening with an internal dimension of 2.05 m (height) × 0.85 m (width). Specific details of the experiments are:

1. For the first experiment (denoted as Exp 1), all openings created by the flutes of ISD2 (18 mm flute height, which is different to ISD1 due to the profile used) were closed with ceramic blanket to simulate a fire scenario with 'no leakages' (Fig. 4).
2. For the second experiment (denoted as Exp 2), all openings created by the flutes of ISD2 were left open to simulate a fire scenario with leakages (Fig. 5). The hypothesis was that leakages will increase fire spread rates since the openings allowed for flame impingement, but might reduce the radiation emitted since more hot gases are allowed to escape the enclosure.
3. Lastly, the third experiment (denoted as Exp 3), was an exact replica of Exp 1, but had a glass pane installed at the window (Fig. 6), and the back 1.4 m × 2.4 m area (relative to Fig. 3) of the roof had polycarbonate sheets (Fig. 6), as opposed to steel sheets. Since the polycarbonate sheets have a low melting point (of approximately 155°C), the polycarbonate sheets will melt as ISD2 ignited, creating a horizontal roof vent. The hypothesis was that as soon as the polycarbonate sheets melted away, the additional ventilation would reduce the external flames from the door opening, which would reduce the likelihood of fire spread. This is building on a concept first introduced by Beshir et al. [16][~~7~~]. Here the effects of both a glass window and polycarbonate sheets are investigated. It is assumed that the window will not affect results for the polycarbonate sheets and vice versa. Since the glass window will only affect the fire behavior up to ignition of ISD 2 and the polycarbonate sheets will only affect the fire behavior once ISD2 is ignited.

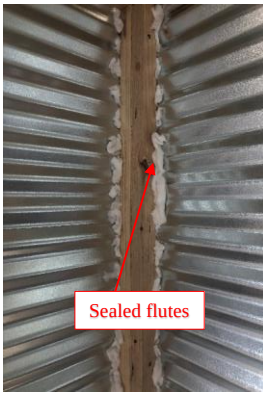

Fig. 4. Closed flutes in ISD2 for Exp 1

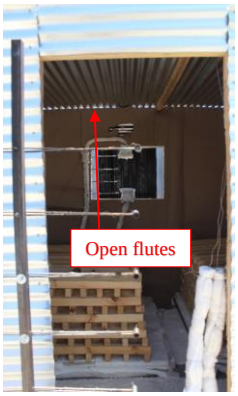

Fig. 5. Open flutes in ISD2 for Exp 2

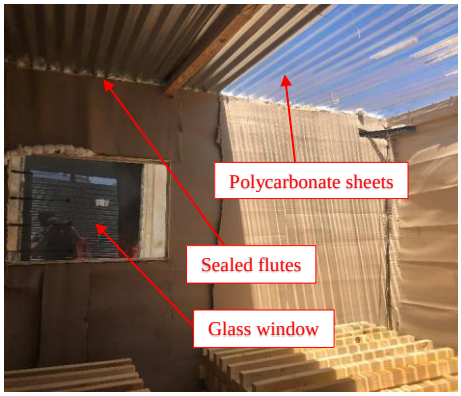

Fig. 6. Polycarbonate sheets and glass window inside ISD2 during Exp 3

Table 1 summarizes the parameters pertaining to ISD2 for the three full-scale experiments considered in this work. ISD1 was exactly the same for all three experiments.

Table 1: Summary of the ISD2 used in full-scale experiment conducted in this work

	Experiment 1 (Exp 1)	Experiment 2 (Exp 2)	Experiment 3 (Exp 3)
Wall material	Corrugated steel sheets	Corrugated steel sheets	Corrugated steel sheets
Lining material	Cardboard	Cardboard	Cardboard
Leakages (Open flutes)	No	Yes	No
Roof vent	None	None	1.4 m × 2.4 m
Glass in window	No (window open)	No (window open)	Yes (3 mm thick)

2.2. Fuel

In reality the fuel load in informal settlement dwellings can range significantly and according to Walls et al. [3][~~3~~], the fuel load can be anything from 400 MJ/m^2 to 2000 MJ/m^2, but this requires further research to be accurately defined. Cicione et al. [6][~~6~~] interviewed a number of firefighters, that fought more than 2000 informal settlement fire combined. These firefighters estimated that the fuel load in ISDs ~~are~~ is higher than that of formal dwellings (an average of 780 MJ/m^2) as stipulated in the EN1991-1-2 [17][~~17~~]. For simplicity and experimental purposes, it was decided to make the fuel load 30 kg/m^2 of timber, that had a calorific value of 17 MJ/kg as measured by the bomb calorimeter, resulting in a fuel load of approximately 510 MJ/m^2. The 200 timber pieces (0.04 m ×0.06 m × 1.2 m) were divided into two timber cribs. Each crib had 10 layers with 10 timber pieces per layer (Fig. 5 and Fig. 6). Using ref. [18][~~18~~], it was estimated that for free burning conditions, these cribs would have a surface-controlled mass loss rate (MLR) limit of 0.39 kg/s combined. However, for burning within an enclosure, the ventilation-controlled MLR is calculated using the following equation [19][~~19~~]:

$$\dot{m} = 0.12 A_o \sqrt{H_o} \quad (1)$$

where A_o is the total area of the openings and H_o is the area-weighted equivalent opening height. For ISD1 and ISD2 the calculated ventilation-controlled MLRs are 0.3 kg/s and 0.355 kg/s (i.e., without accounting for the roof vents or leakages), respectively. The cribs were placed 200 mm from the left long wall of each dwelling, 400 mm from the short walls and 400 mm apart, as depicted in Fig. 3. As mentioned earlier, ISD1 had no cardboard lining for all 3 experiments, but ISD2 had cardboard lining for all experiments (Fig. 5 and Fig. 6) in order to mimic the highly flammable cladding and contents present in many real ISDs [6][~~6~~].

2.3. Measurements

All gas temperatures were recorded using 1.5mm diameter Type K thermocouples (TCs). The incident heat fluxes emitted by the dwellings were captured using Thin Skin Calorimeters (TSCs), that were calibrated against a water-cooled heat flux gauge. Both the TSC and TC readings were recorded with an Agilent 34980A data logger at a frequency of 0.2 Hz. The external reference temperature was recorded with a 4-wire resistance temperature detector (RTD). Flow velocities were measured at the door and window openings using Bi-directional Flow Probes (FPs) and MLRs were recorded for each timber crib by placing each crib on a 1.2 m × 1.2 m scale with a 10 g accuracy. Wind speed and direction were measured using a hemispherical cup-type anemometer, placed approximately 10 m away from the experimental setup at a height of 2 m. All voltage output data was recorded at a frequency of 1 Hz. Fig. 7 depicts the positions of all TSCs, TCs, FPs and scales. The number next to the instrumentation abbreviation indicates the number of instruments in a particular equipment tree (e.g., TCx, where x is the number of TCs at that position). Fig. 8 depicts the spacing of each equipment tree used in these experiments.

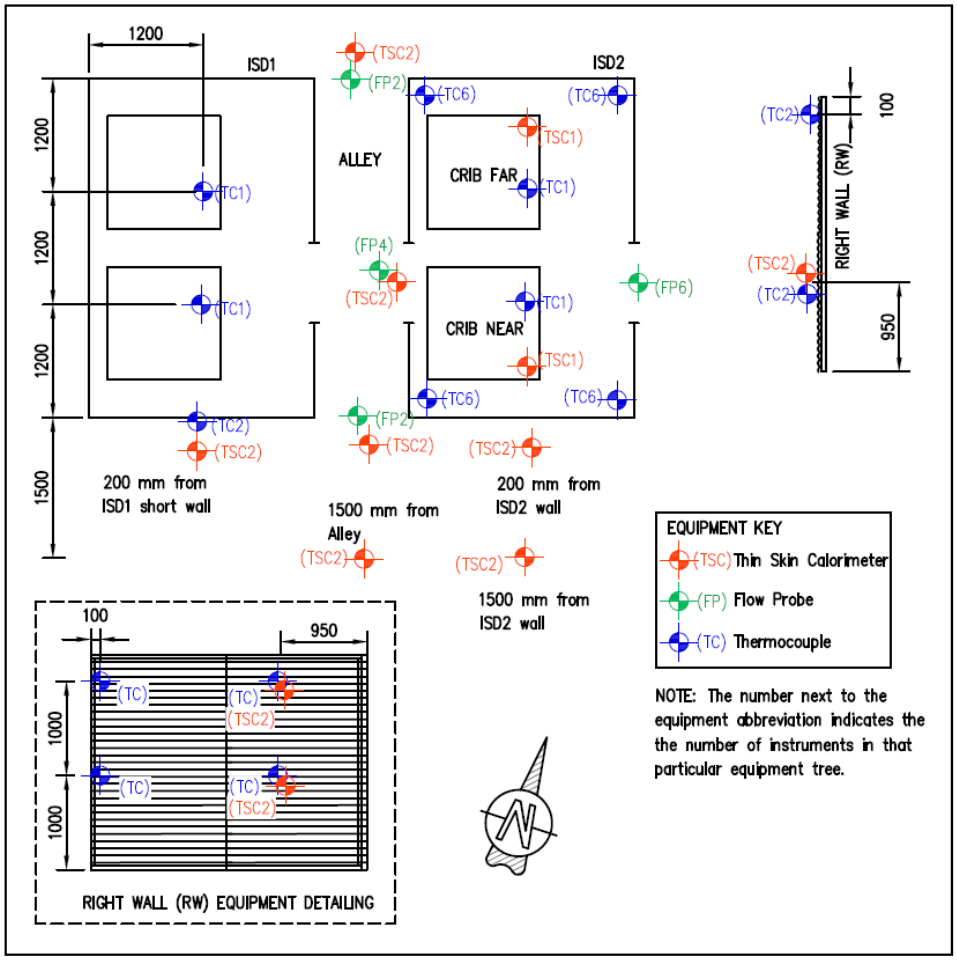

Fig. 7. Equipment layout (top), equipment key (middle right), and right wall detailing (bottom left)

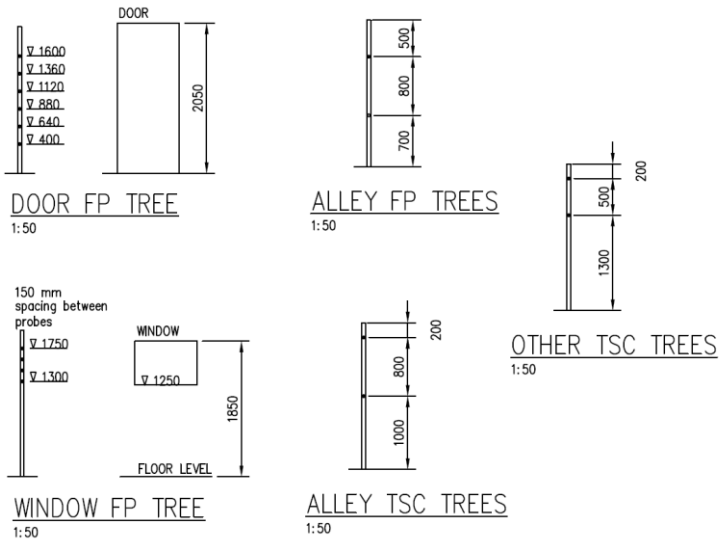

Fig. 8. Instrumentation heights for the various equipment trees

3. B-RISK SETUP OF EXPERIMENTS CONDUCTED

In this work, B-RISK [20], a two-zone model software, is used to simulate the experiments conducted and to further investigate the effect of leakages and ventilation on ISD fire dynamics through a parametric study. In this section the simulation setup of the three experiments conducted, denoted as Exp 1, Exp 2 and Exp 3, are discussed. The numerical results are presented alongside the experimental results in the sections that follow. Only ISD2 was simulated in B-RISK for each experiment, since the ventilation or leakage changes only occurred in ISD2, with ISD1 being exactly the same for all three experiments. The ISD2 dwelling size was used for the volumetric domain size in B-RISK ("Room Design" in B-RISK), and the combustion properties used for the timber cribs (simulated as an item under "Fire Specification" in B-RISK) were those noted in section 2.2 above. Cardboard lining was ignored since it only contributed towards the fire for a few seconds (discussed below) and only the mass loss rates of the cribs was measured in the experiments. A soot yield of 0.015 g/g, CO2 of 1.33 g/g and radiant loss fraction χ_R of 0.3 were taken from Table 3-4.14 of the SFPE Handbook [21]~~[20]~~. The heat of gasification (1.8 kJ/g) has been selected from Table 3-4.7 of the SFPE Handbook [21]~~[21]~~, based on similar representative materials. Assuming a combustion efficiency of 1, the effective heat of combustion equals the gross heat of combustion (17 kJ/g) of the timber used in these experiments. All sheets were assumed to be flat in B-RISK since corrugated sheets cannot be simulated in B-RISK. Additionally, leakages created by the corrugated flutes (Exp 2) were assumed to be regular openings with the same opening size as in the experiment, located at the top of the walls (i.e., assuming the flute opening to be 9 mm high in B-RISK). A summary of the inputs to the B-RISK scenarios are listed in Table 2.

Table 2: Summary of B-RISK inputs

Model Name	Corresponding Experiment	Heat release rate curve used	Ventilation and Geometry details
Scenario 1	Exp 1	HRR curve of Exp 1 as depicted in Fig. 13 b)	The exact geometry and ventilation conditions as described in Fig. 3, Fig. 4 and Table 1
Scenario 2	Exp 2	HRR curve of Exp 2 as depicted in Fig. 13 b)	The exact geometry and ventilation conditions as described in Fig. 3, Fig. 5 and Table 1
Scenario 3	Exp 3	HRR curve of Exp 3 as depicted in Fig. 13 b)	The exact geometry and ventilation conditions as described in Fig. 3, Fig. 6 and Table 1

Since B-RISK is a zonal model software, external wind conditions cannot be simulated (this is one limitation of zone modelling), hence wind was not simulated in any of the B-RISK scenarios.

4. EXPERIMENTAL RESULTS AND DISCUSSION

For Exp 1 (no leakages – i.e. closed flutes), depicted in Fig. 9 a) and b), ISD1 reached a fully developed fire stage within 3.9 minutes after ignition. At this point, flames emerged out of the door, pushing hot gases into ISD2. From a water-cooled camera placed within ISD2, one could see flames pulse through the window every few seconds. Seconds before the ignition of ISD2, the gas temperature of the hot layer inside ISD2 reached a uniform temperature of approximately 164-174 °C from ceiling level to approximately 2.05 m from ground level (this is the height of the door). At approximately 5.4 min the cardboard lining (above the window) of ISD2 ignited, and as a result of the preheating, rapid fire spread across the surface of the cardboard ensued horizontally, then down, leading to flashover and a fully developed stage that was attained within 1.5 minutes. Note that flashover in this paper refers to a rapid transition period between the growth phase and the fully developed phase, as opposed to a single point of transition.

Fig. 9 a) Visually depiction of Exp 1

Fig. 9 b) Inside view through the door of ISD2 for Exp 1

For Exp 2 (leakages – i.e. open flutes), depicted in Fig. 10 a), ISD1 reached a fully developed fire stage within 3.9 minutes. At this point, flames already emerged out of the door, pushing hot gases into ISD2. From a water-cooled camera inside ISD2, one could see flame pulse through the window every few seconds, as per Exp. 1. Seconds before the ignition of ISD2 the gas temperature of the hot layer inside ISD2 reached a uniform temperature of approximately 90-115 °C from ceiling level to approximately 2.05 m from ground level. At approximately 5.3 min the cardboard lining of ISD2 ignited (Fig. 10 b)), and as a result of the preheating, rapid fire spread across the surface of the cardboard ensued (horizontally, then vertically down), leading to flashover and a fully developed stage that was attained within 2 minutes.

Fig. 10 a) Visually depiction of Exp 2

Fig. 10 b) Ignition of the cardboard lining in ISD2 for Exp 2

For Exp 3 (roof vent), after ignition, ISD1 reached a full developed fire stage within 4.2 minutes. At this point, flames already emerged out of the door, pushing hot gases into ISD2. From video footage inside the door of ISD2, one could see the glass window cracking at about 3 minutes (from ignition of ISD1), partial fallout at about 3.5 minutes and complete fallout at approximately 8 minutes (although complete fallout is difficult to visually identify in the video footage). Seconds before the ignition of ISD2 the gas temperature of the hot layer inside ISD2 reached a uniform temperature of approximately 50 °C from

ceiling level to approximately 2.05 m from ground level. At approximately 5 minutes the cardboard lining of ISD2 ignited. The heat from the burning cardboard rapidly melted the polycarbonate sheets as depicted in Fig. 11 a) to d). A fully developed stage was attained within approximately 3.7 minutes after ignition.

Fig. 11 a) Ignition of ISD2

Fig. 11 b) Early spread of flames across the cardboard surface and the polycarbonate sheets starting to melt

Fig. 11 c) Visual illustration of the melting of the polycarbonate sheets

Fig. 11 d) Polycarbonate sheets almost completely melted away

Table 3 summarizes the details pertaining to ignition, flashover and flame spread for Exp 1 – Exp 3 as discussed above.

Table 3: Summary of Exp 1 - Exp 3. Note that the percentages in brackets show the percentage increase (+) or decrease (-) compared to Exp 1.

	Exp 1 (closed flutes)	**Exp 2 (Open flutes)**	**Exp 3 (Glass window – polycarbonate roof sheets)**
Ventilation	Open door and window (flutes closed)	Open door, window and flutes	Open door. Glass window. Polycarbonate sheets roof (flutes closed)
Time to fully developed fire stage in ISD1 [minutes]	3.9	3.9 (0%)	4.2 (+7.7%)
Hot layer temperature prior to ignition of ISD2 [°C]	164-174	90-115 (-45%)	45-50 (-73%)
Time-to-ignition of ISD2	5.4	5.3 (-1.85%)	5.0 (-7.4%)

[minutes]			
Ignition to fully developed stage in ISD2 [minutes]	1.5	2 (+33%)	3.7 (+147%)
Average HRR of ISD2 for the first 2 minutes after the fully developed fire stage was reached [MW]	6.2	7.2 (+16%)	8.7 (+40%)
Average heat flux to the top of the RW over any 2 minutes that gives the highest average (before structural collapse) [kW/m^2]	38	39 (+2.6%)	31 (-18%)
Maximum incident heat flux on to RW [kW/m^2]	52	59 (+13%)	39 (-25%)
Maximum horizontal flame length from door opening (based on video footage) [meters]	2.2 m	2 m (-9%)	0.2-0.4 m (-82%)

Based on the data in Table 3, it is clear that the glass window panel and open or closed flutes had no effect on the fire spread rate for this experimental configuration (door to window fire spread), as the window opening was dominant in controlling fire spread. Once ISD2 ignited, the ventilation clearly had a substantial effect on the time to flashover. Exp 1 had the least openings and thus experienced the largest amount of heat buildup with a hot layer temperature of approximately 164-174°C in ISD2, prior to ignition. Exp 2 experienced almost exactly the same time to flashover as Exp 1, even with open flutes. However, the hot gases were able to escape more easily, resulting in a slightly lower hot layer temperature of around 90-115°C in ISD2, prior to ignition. The glass installed in ISD2 for Exp 3 significantly reduced the amount of hot gases entering ISD2 and, as a result, the hot gas layer temperature in ISD2 was below 50°C prior to ignition. From the video data, it is clear that fire spread rate across the surface of the cardboard lining were faster for the experiments where the hot layer temperature was higher prior to ignition. Although obvious, it shows that dwelling configurations with less ventilation at ceiling level will trap the hot gases better, which will increase that rate at which the lining material preheats, allowing for faster fire spread across the cardboard lining, that as a result, leads to the onset of flashover occurring faster. Additionally, an enclosure with lower ventilation would require a lower HRR for flashover to occur [22][~~22~~]. Hence, less ventilation increases the spread rate over the surface of the lining material and at the same time reduces the HRR needed for the onset of flashover.

Fig. 12 a) to c) depict the wind direction and wind speed during Exp 1 to Exp 3, respectively. A wind direction of 0° indicates an east wind with a clockwise rotation being positive (Fig. 3). The wind data was captured approximately 10 m away from the experiments (to exclude fire-induced flows from the measurements), towards the bottom left corner of Fig. 3, at a height of 2 m using a hemispherical cup-type anemometer.

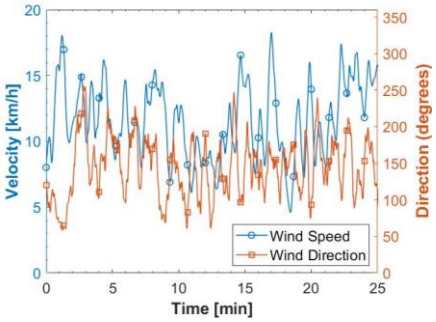

Fig. 12 a) Wind speed and direction during Exp 1

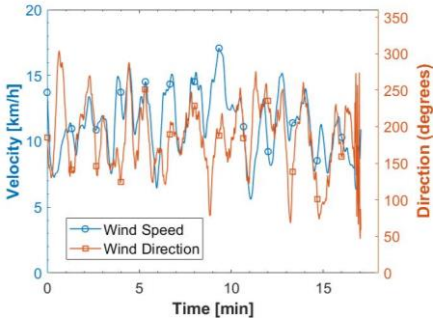

Fig. 12 b) Wind speed and direction during Exp 2

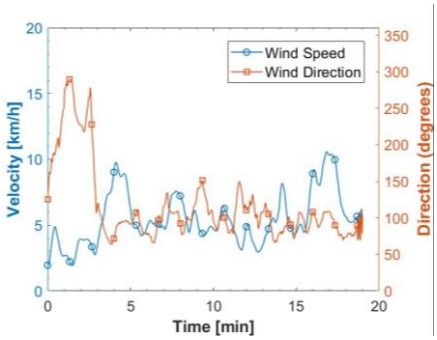

Fig. 12 c) Wind speed and direction during Exp 3. A wind direction of 0° indicates an east wind with a clockwise rotation being positive.

4.1. Heat release rates

Fig. 13 a) and b) depict the heat release rates of ISD1 and ISD2 for Exp 1 to Exp 3, respectively, based on the MLR from the scales. For the positioning of the scales refer to Fig. 7.

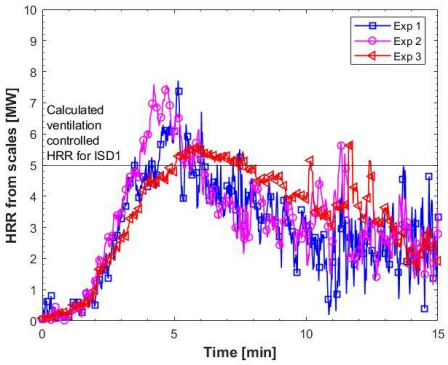

Fig. 13 a) HRRs of ISD1 as indirectly measured by the scales

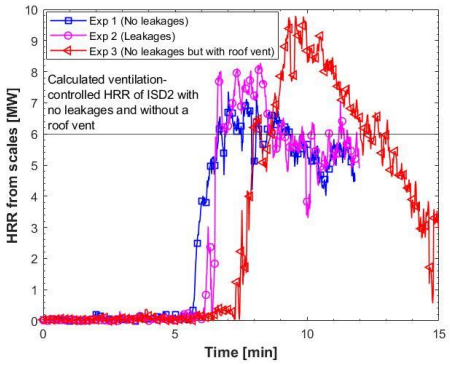

Fig. 13 b) HRRs of ISD2 as indirectly measured by the scales

For ISD2 (Exp 3), the polycarbonate sheets created a large opening meaning that the enclosure was not ventilation-controlled and that the mass loss rates of the cribs should be limited by the crib geometry. According to Babrauskas [23]~~[23]~~ the mass loss rate of a free burning crib can be either porosity-controlled or surface-controlled. The HRR of the free burning cribs can then be estimated by the following very well-known HRR formula:

$$\dot{Q} = \dot{m}\Delta H_{eff} \tag{2}$$

where $\dot{m}$ is the mass loss rate [kg/s] and ΔH_{eff} is the effective heat of combustion [kJ/kg]. The mass loss rate, i.e. of the free burning cribs, is taken as the lesser of the surface-controlled mass loss rate:

$$\dot{m} = \frac{4}{D} m_0 v_p \left(1 - \frac{2 v_p t}{D}\right) \tag{3}$$

and porosity-controlled mass loss rate:

$$\dot{m} = 4.4 \times 10^{-4} \left(\frac{S}{h_c}\right)\left(\frac{m_0}{D}\right) \tag{4}$$

where the stick thickness is D = 0.04 m, the clear spacing is S = 0.09 m, the crib height is h_c = 0.6 m, the number of sticks per row is n = 10, the initial crib mass was m_0 = 130 kg, giving $v_p = 2.2\times10^{-6}D^{-0.6}$ according to Babrauskas [19]~~[24]~~ and the heat of combustion of the timber is $\Delta Heff$ = 17 MJ/kg (as measured by a bomb calorimeter test and assuming a combustion efficiency of 1). In this case, there were 2 cribs, thus the mass loss rate is multiplied by 2 to give the total HRR. Substituting all the knowns into Equation 3 and Equation 4, the porosity-controlled HRR is calculated as 7.2 MW and the surface-controlled HRR is calculated as 6.7 MW. Implying that the free burning crib will have an absolute maximum HRR, that is surface-controlled, of 6.7 MW. However, in Fig. 13 b) it is clear that the HRR of the cribs exceeded the surface-controlled HRR and

even exceeded the porosity-controlled HRR. This is most likely because for Exp 3 we have forced flow through the cribs due to air entrainment, i.e. higher velocities than normal created by a so called 'chimney effect'. This is evident when we consider the inward gas velocities measured by the door flow probes. For Exp 1 and 2, the maximum inward gas velocity is approximately 2 m/s, where the maximum inward gas velocity for Exp 3 is approximately 4 m/s. This is discussed in more detail in the sections that follow.

Considering Exp 1, it can be seen that the calculated surface-controlled HRR of the cribs of approximately 6.7 MW, corresponds relatively well with the total MLR measured by the scale. The maximum measured HRR is approximately 7.6 MW for ISD1 and 7.2 MW for ISD2. Equation 1 gives a ventilation limited fire of about 6 MW within the dwelling. The remaining energy release rate, $7.6 - 6 = 1.6$ MW for ISD1 and $7.2 - 6 = 1.2$ MW for ISD2, must then burn outside of the dwellings. This is clear when comparing the flame lengths of ISD1 and ISD2 (Fig. 9). From video footage, it is clear that a large volume of flames emerges from ISD1 compared to ISD2, as depicted in Fig. 9.

4.2. Gas temperatures

Fig. 14 a) to d)Fig. depict the temperature profile across the height of ISD2 for Exp 1 and the B-RISK scenario 1 (scenario 1 corresponds to Exp 1) at the left back, right back, right front and left front, respectively. The thermocouples were labelled from TC6 to TC1, with TC6 being at the top and TC1 being at the bottom of the TC tree. The TCs were placed at the following heights, from floor level, for each tree: 2.2 m, 2.15 m, 2.05 m, 1.9 m, 1.7 m and 1.55 m. The reason the thermocouples were more concentrated in the top part of the dwelling was because the authors were interested in the smoke layer development before flashover to understand the preheating in the second dwelling. These graphs are only plotted up to structural collapse, which occurred at approximately 12.4 minutes after ignition of ISD1. As mentioned earlier, during Exp 1, seconds before ignition of ISD2 the gas temperature of the hot layer inside ISD2 reached a uniform temperature of approximately 164-174 °C from ceiling level to approximately 2.05 m from ground level (this is the height of the door).

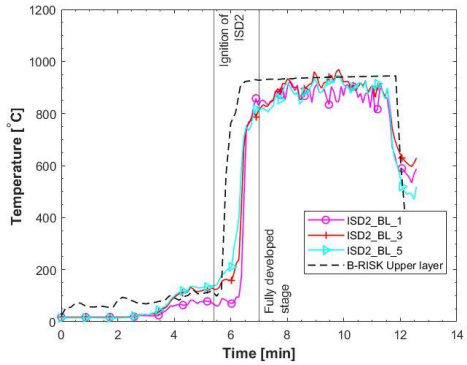

Fig. 14 a) Back left thermocouple tree of ISD2 for Exp 1 and B-RISK

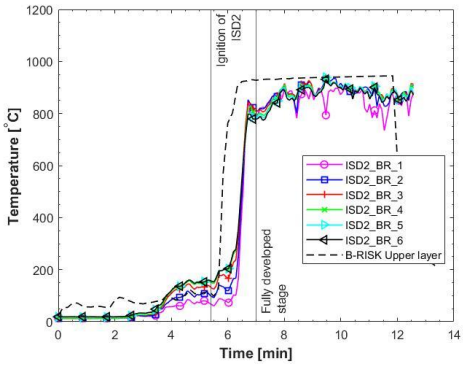

Fig. 14 b) Back right thermocouple tree of ISD2 for Exp 1 and B-RISK

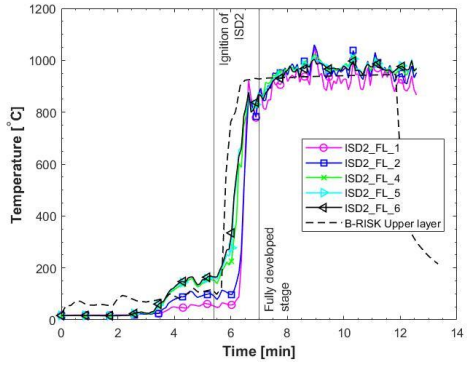

Fig. 14 c) Front left thermocouple tree of ISD2 for Exp 1 and B-RISK

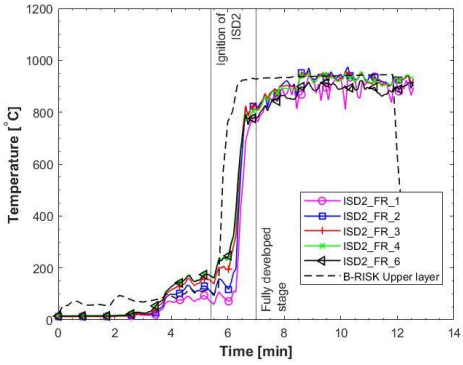

Fig. 14 d) Front right thermocouple tree of ISD2 for Exp 1 and B-RISK

Fig. 15 a) to Fig. d) depict the temperature profile across the height of ISD2 for Exp 2 and the B-RISK scenario 2 at the left back, right back, right front and left front, respectively. The thermocouples were labelled and spaced the same as Exp 1. Similar to Exp 1, the graphs are only plotted up to structural collapse that occurred at approximately 12.4 minutes after ignition of ISD1 (which just happens to be the same as Exp 1).

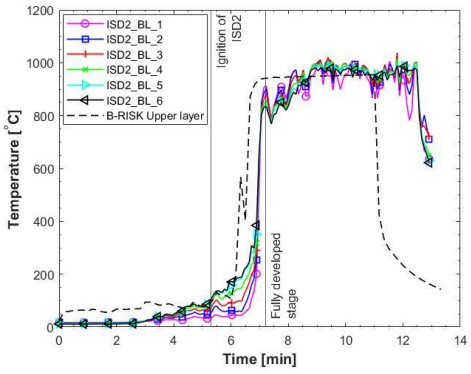

Fig. 15 a) Back left thermocouple tree of ISD 2 for Exp 2 and B-RISK

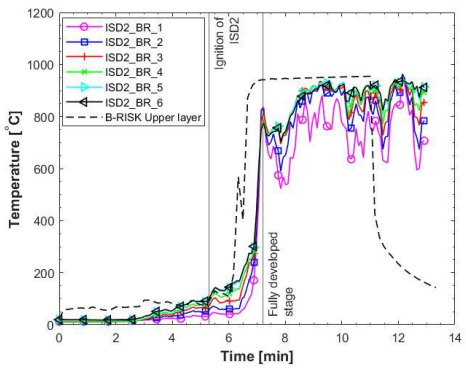

Fig. 15 b) Back right thermocouple tree of ISD 2 for Exp 2 and B-RISK

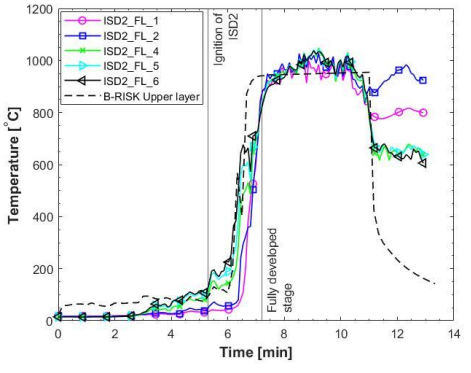

Fig. 15 c) Front left thermocouple tree of ISD 2 for Exp 2 and B-RISK

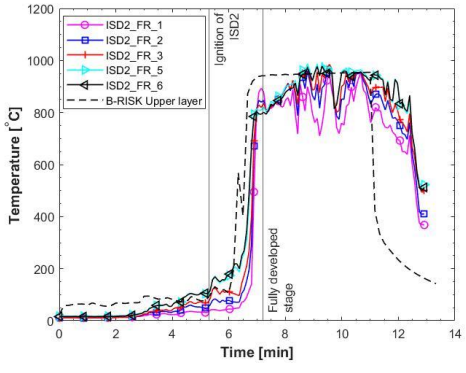

Fig. 15 d) Front right thermocouple tree of ISD 2 for Exp 2 and B-RISK

Fig. 16 a) to d)Fig. depict the temperature profile across the height of ISD2 and the B-RISK scenario 3 at the left back, right back, right front and left front, respectively. The thermocouples were labelled and spaced the same as Exp 1 and Exp 2. These graphs are only plotted up to structural collapse that occurred at approximately 16 minutes after ignition of ISD1.

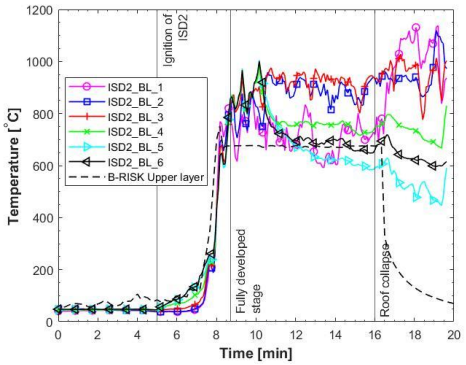

Fig. 16 a) Back left thermocouple tree of ISD 2 of Exp 3 and B-RISK

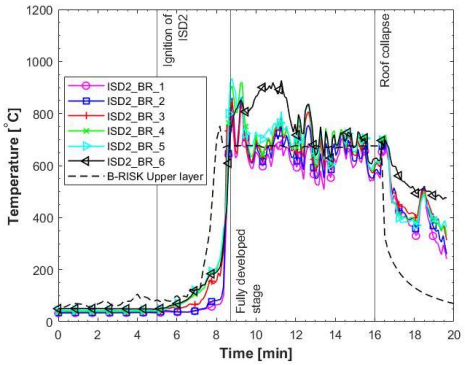

Fig. 16 b) Back right thermocouple tree of ISD 2 of Exp 3 and B-RISK

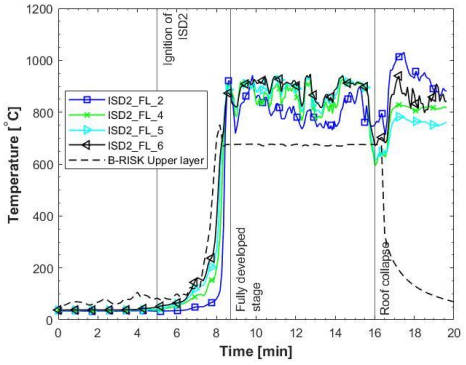

Fig. 16 c) Front left thermocouple tree of ISD 2 of Exp 3 and B-RISK

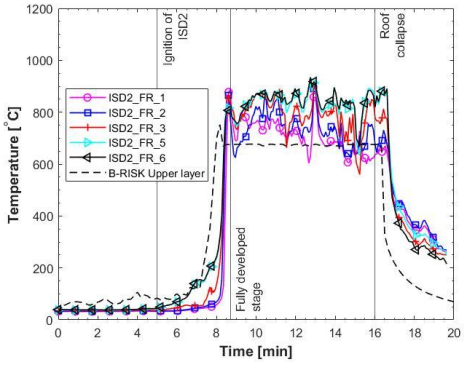

Fig. 16 d) Front right thermocouple tree of ISD 2 of Exp 3 and B-RISK

Considering Fig. 14 to Fig. 16, it is clear that B-RISK captures the time-temperature development within these dwellings sufficiently well. It appears that B-RISK slightly underpredicts the time to flashover for these dwellings, with the deviation in time to flashover being less than 10% in all cases. The maximum temperatures reached during the fully developed stage are very similar to that expected for formal dwellings of just below 1000 °C on average for Exp 1 and Exp 2 and around 600-800 °C for Exp 3 (depending if one considers the front or back temperatures). The maximum temperatures are captured extremely well by B-RISK with the only significant deviations being in Exp 3 at the front of the dwelling. It should be noted that for this zone model only the area of the roof vent is accounted for and not the location of the roof vent. The gas temperatures are then averaged out across the hot layer (upper layer in B-RISK). Hence, B-RISK captures the temperature relatively well at the back ISD2 for Exp 3, where the vent was actually located, but does however miss the slight heat build-up at the front of the dwelling where the corrugated steel roof is still present.

4.3. Gas flow velocities at openings

Fig. 17 and Fig. 18 depict the flow velocities of ISD2 for Exp 1 and for B-RISK scenario 1 at the door and window, respectively.

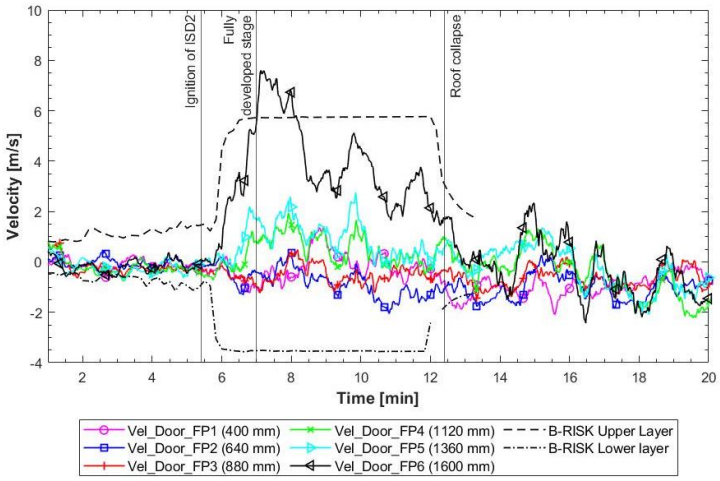

Fig. 17. Flow velocity data at the door of ISD2 for Exp 1 and B-RISK with positive velocity indicating flow out of the dwelling

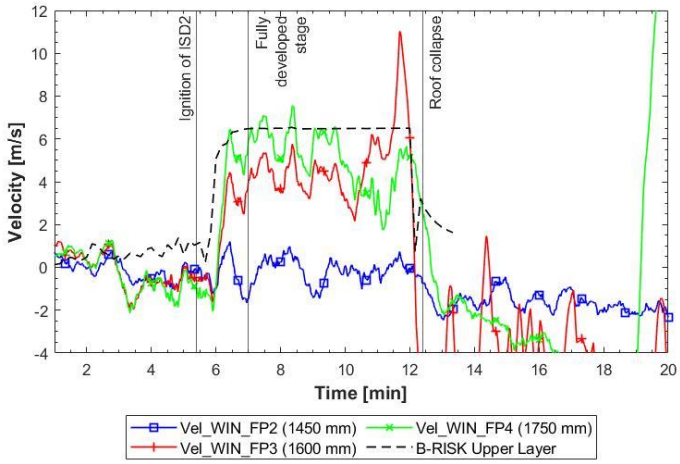

Fig. 18. Flow velocity data at the window of ISD2 for Exp 1 and B-RISK with positive velocity indicating flow out of the dwelling

Considering the experimental door velocities (Fig. 17), the neutral plane is between 900 mm - 1000 mm, which is similar to the 901 mm estimated by B-RISK during the fully developed fire stage. The gas flow velocity out of the window (Fig. 18) is slightly overpredicted by B-RISK. However, there are large discrepancies between the experimental and numerical gas velocities across the door opening (Fig. 17). For the hot gases leaving the enclosure, the discrepancy is likely as a result of the experimental outside pressure fluctuating significantly as the wind speed and direction fluctuates (Fig. 12 a)). For the cold air entering the enclosure, it is clear that B-RISK overestimates the mass flow of air into the enclosure. It is not clear why there is such a large discrepancy between the experimental and numerical results here. Based on a neutral plane height of 900 mm, one can calculate the maximum expected velocity of air entering the enclosure using the following equation [24][~~25~~]:

$$V_{a,max} = \sqrt{\frac{2H_N(\rho_a - \rho_g)g}{\rho_a}} \quad (5)$$

where H_N is the height of the neutral plane (0.9 m in this case), ρ_a is the density of air (assumed to be 1.2 kg/m^3 in this case), ρ_g is the density of the hot gases (assumed to be 0.4 kg/m^3 based on the ideal gas theory) and g is the gravitational acceleration constant. Hence, in this case it is expected that the maximum velocity entering the enclosure should be approximately 3.43

m/s, which seems to correspond well with B-RISK. It does appear that the measurements might be under-quantifying the amount of air entering the dwelling (since air is needed for burning to occur). This could potentially be linked to the leakages allowing air to enter at other places. A plausible explanation could be that air is being sucked in all around the perimeter of the dwelling between the bottom of the dwelling and the floor, since the dwellings were merely placed on the floor. Hence, any eccentricities would have created some gaps for air to enter.

Fig. 19 and Fig. 20 depict the flow velocities at the door and window of ISD2 for Exp 2, respectively.

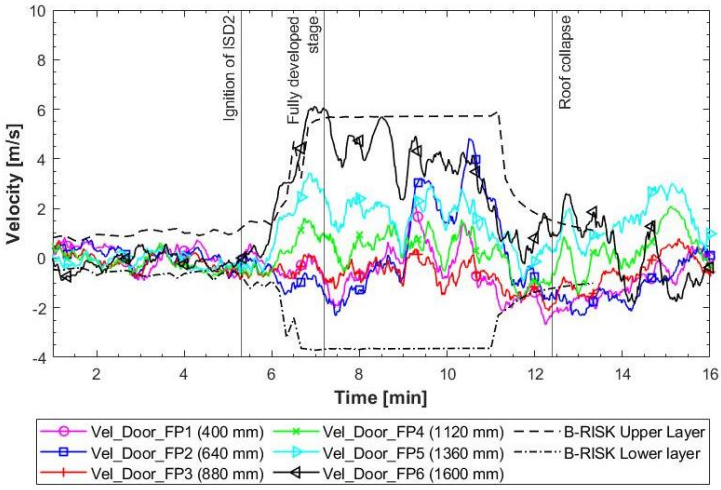

Fig. 19. Flow velocity data at the door of ISD2 for Exp 2 with positive velocity indicating flow out of the dwelling

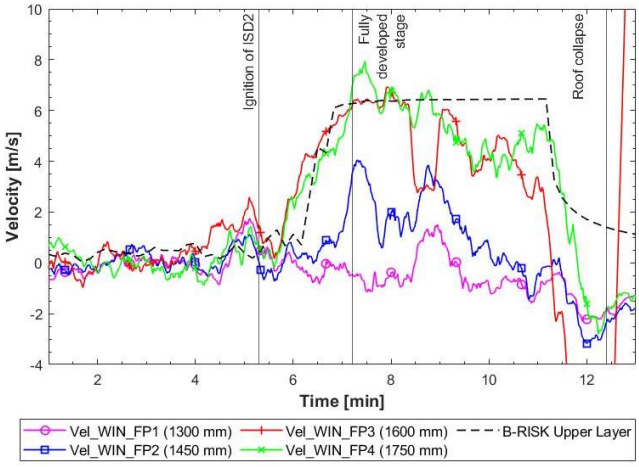

Fig. 20. Flow velocity data at the window of ISD2 for Exp 2 with positive velocity indicating flow out of the dwelling

Considering Fig. 19 and Fig. 20 it is clear that B-RISK captures the trend of the hot gas velocities leaving the dwelling relatively well. Where, similar to above, the deviations can be explained but the fluctuations in wind speed and directions during the experiment (B-RISK cannot account for wind as mentioned before). Similar to Exp 1, B-RISK overpredicts the amount of air entering the enclosure compared to the experimental results. The window velocities (Fig. 20) indicate that the neutral plane of ISD2 for Exp 2 should be at approximately 1300-1350 mm, since the velocities at Vel_WIN_FP1 approximately zero. This is similar to the 1400 mm predicted by B-RISK. However, considering the door velocities (Fig. 19), the neutral plane is approximately 900 mm, which is similar the neutral plane measured during Exp 1. Similar to Exp 1, it is plausible considering the outside pressure at the window (i.e., wind funneling though alley, hot gases pushing from ISD1 to

ISD2, etc.) are different than the outside pressure at the door of ISD2 and this phenomenon (i.e., wind changing the outside pressures) will not be captured in B-RISK as a result of the software's inability to simulate wind.

Fig. 21 and Fig. 22 depict the flow velocities at the door and window of ISD2 for Exp 3, respectively.

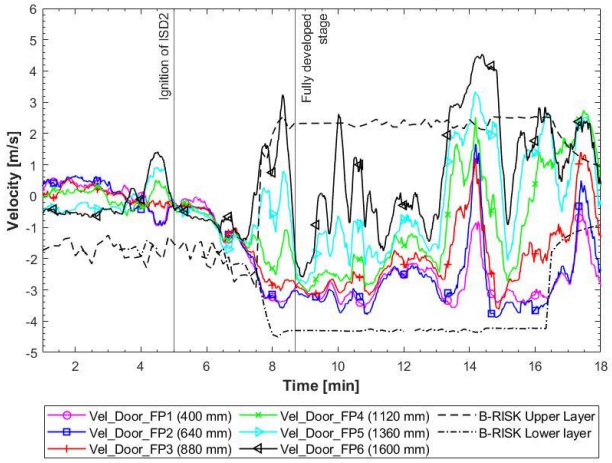

Fig. 21. Flow velocity data at the door of ISD2 for Exp 3 with positive velocity indicating flow out of the dwelling

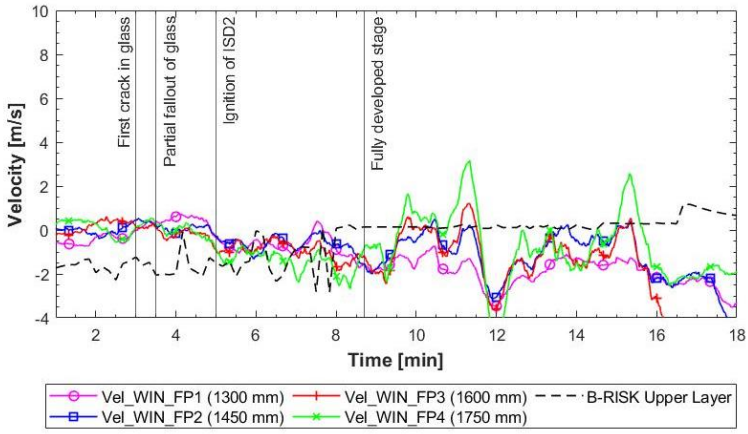

Fig. 22. Flow velocity data at the window of ISD2 for Exp 3

Considering Fig. 21 and Fig. 22 it is clear that the flow out of the door and window was significantly reduced for Exp 3 as a result of the new vent created in the roof opening. It was observed that almost no flames emerged out of the door (Fig. 23 a)) but that approximately all flames were out of the roof vent (Fig. 23 b)). The roof vent also significantly increased the airflow into the dwelling, which is clear by the high inward velocities (Vel_Door_FP1), which increased the amount of oxygen to the cribs and as a result significantly increased the total HRR of the cribs Fig. 13 b). The B-RISK results compare well with the overall trend, however similar to Exp 1 and Exp 2, the software did overpredict the mass flow of air into the enclosure compared to the experiment (however in this case it is closer to the experimental values compared to Exp 1 and Exp 2). Additionally, there are no fluctuations in the B-RISK results, which again is as a result of the software's limitation to simulate wind.

Fig. 23 a) Reduction in flame length emerging out of door for Exp. 3

Fig. 23 b) Flames through roof vent of Exp. 3

4.4. Incident radiation emitted from ISD2

Considering Fig. 14 and Fig. 16, it is clear that adding the roof vent at ceiling level reduced the gas temperatures within ISD2 of Exp 3. Since temperature affects radiation emitted to the power of 4, it is clear that the radiation emitted by the hot gases inside ISD2 for Exp 3 through the door opening will be significantly less compared to ISD 2 for Exp 1 and 2 (since the gas temperature inside ISD2 for Exp 3 is significantly less than Exp 1 and 2). This was evident with the heat fluxes measured at the RW during each experiment, as depicted in Fig. 24.

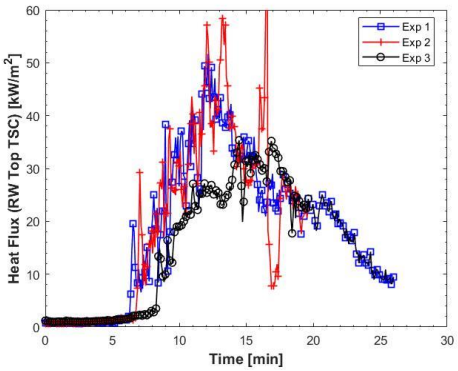

Fig. 24. Heat flux reordered by the top TSC (2 m from ground level) of the RW (2 m for ISD2)

From Fig. 24 it can be seen that the incident heat flux received by the RW peaks at about 50 kW/m^2 for Exp 1. For Exp 2, the incident heat flux received by the RW peaks at about 60 kW/m^2. Although Exp 2 peaks higher than Exp 1, the general heat flux curves between the 2 experiments are relatively similar. For both Exp 1 and Exp 2, a slight peak in heat flux occurs seconds before the fully developed fire stage is reached (i.e., at approximately 6-7 minutes), corresponding to the time where the cardboard lining was engulfed in flames. For Exp 3, the incident heat flux received by the RW peaks just below 35 kW/m^2, with the general heat flux curve being approximately 10-20 kW/m^2 less than Exp 1 and 2. Hence, it can be seen that adding a roof vent (Exp 3) approximately reduced both the average incident heat flux and maximum incident heat flux received at the RW by approximately 25% compared to Exp 1 and Exp 2. Thus, changing the ventilation conditions will affect the radiation emitted and hence will increase or decrease fire spread from one dwelling to another. In addition to the reduction in gas temperature when adding a roof vent, it is clear from experimental observation that the flame lengths ejecting from the door and window significantly reduces, i.e. 2.2 m for Exp 1 (no roof vent) versus 0.4 m for Exp 3 (with roof vent), as listed in Table 3~~2~~. Hence, this further reduces the risk of fire spread in the direction of flames emitted from the door since the probability for flame impingement onto the neighboring dwellings is reduced. This reduction in flame length is strongly linked to the movement of the neutral plane. Increasing the ventilation increases the height of the neutral plane, which results in

lower gas flow velocities exiting the dwelling. However, now a large fire plume ejects from the roof (see Fig. 23 b)) of ISD2 for Exp 3, which now radiates in all directions. This means that there are potential new fire spread pathways in multiple directions which could auto-ignite items if close enough.

The predictive capabilities within B-RISK can be used to indirectly estimate how much radiation is emitted by this fire plume ejecting from the roof. Fig. 25 depicts the B-RISK predicted incident radiation that falls onto the inner wall of the dwelling for ISD2. This can also be seen as the radiation intensity at the door of the dwelling as a result of the hot gases. In other words, if one assumes that the door opening acts as a radiant panel (hot gases being the source of heat), the radiation depicted in Fig. 25 is the radiation at the door opening (excluding the external flames). Hence, we can now calculate the radiation component of the hot gases at two meters away from the door (where the TSC was located in the experiment) using a configuration factor between the door opening and the TSC location at the RW (located 2 m away from ISD2 at a height of 2 m from the ground, in front of the door).

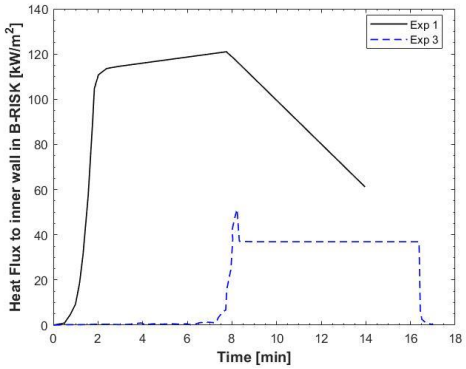

Fig. 25. Incident radiation to inner wall in B-RISK, which can be seen as the radiation intensity at the door.

The configuration factor (otherwise known as a view factor) for this scenario is equal to 0.32 (configuration factor was calculated as done in ref. [12][~~12~~]), implying that the maximum radiation received by the TSC at 2 m away from the door as a result of the hot gases in ISD2 was 38.4 kW/m^2 for Exp 1 and 15.0 kW/m^2 for Exp 3, based on the B-RISK predictions. Comparing these values to the maximum heat fluxes depicted in Fig. 24 of 50 kW/m^2 for Exp 1 and 35 kW/m^2 for Exp 3, one can estimate the radiation component of the flame ejecting from the door of Exp 1 and for the flame ejecting from the roof vent in Exp 3 (assuming the radiation component of the steel sheets are negligible at 2 m – which is what was found in ref. [12][~~12~~]). For Exp 1, the radiation received at 2 m away from the door as a result of the door flame is thus 50 kW/m^2 (measured value) minus 38.4 kW/m^2 (gas component as predicted by B-RISK), which gives 11.6 kW/m^2. For Exp 3, the radiation received at 2 m away from the door as a result of the flame emerging from the roof (no flames from the door in this case, hence one can safely assume the radiation from the door flame is 0 kW/m^2) is thus 35 kW/m^2 (measured value) minus 15.0 kW/m^2 (gas component as predicted by B-RISK), which gives 20.0 kW/m^2. This implies that although adding the roof vent reduced the radiation measured in front of the door opening, compared to Exp 1, it increases the radiation emitted in all other directions by approximately 20 kW/m^2 at 2 m away from the edge of the flame emerging from the roof, which is sufficient to ignite most common combustible materials, assuming a piloted source is present. In a dense settlement adjacent homes within 1-2m often have thin plastic linings, newspaper draft stoppers, hanging washing or other~~s~~ materials at roof level which may ignite readily due to their low thermal inertia and ignition temperatures. Furthermore, large IS conflagrations typically occur during high wind conditions, which would cause flames emerging from roofs to tilt towards adjacent dwellings.

Given the diversion of the external flaming from horizontal openings to the roof opening, it is much less likely that areas of high radiation are spatially incident with a flame to cause piloted ignition. Therefore, the scenario becomes a trade-off between piloted ignition adjacent to openings, and auto-ignition in other areas. Auto-ignition is a complex phenomenon and there are few, if any, comprehensive studies which directly compare auto-ignition heat fluxes or temperatures with corresponding piloted ignition properties for multiple materials. A recent summary of previous studies concluded that critical heat fluxes of wooden materials range from 10-13 kW/m^2 under piloted conditions, but are significantly higher at 25-33 kW/m^2 under auto-ignition conditions [25][~~26~~]. Another study of wooden materials found that under medium level heat fluxes, where auto-ignition could occur, it may still take over 200 seconds longer than under piloted conditions at the same flux [26][~~27~~].

4.5. Radiation to floor level of ISD2

During each experiment, one TSC was placed on each crib in ISD2 to measure the radiation to the cribs as a result of (i) the hot gases before the cardboard ignited and (ii) the radiation to the cribs after the cardboard ignited. The crib TSCs were 700 mm from the floor (i.e.~~,~~ the crib plus scale plus scale protection height). Fig. 26 depicts the incident radiation to the wood

cribs for Exp 1, 2 and 3. The TSC placed on the front crib of ISD2 in Exp 1 broke and gave invalid readings. Thus, only the back crib incident heat flux is depicted in Fig. 26 for Exp 1. It should be noted that the extension cable of the TSCs are only rated to 200°C, although also protected in ceramic blanket, once flashover commences the cables inside the dwelling will still melt and the data afterwards should be ignored in this case. Fig. 27 depicts the incident radiation to floor lever for Exp 1, 2 and 3 predicted by B-RISK.

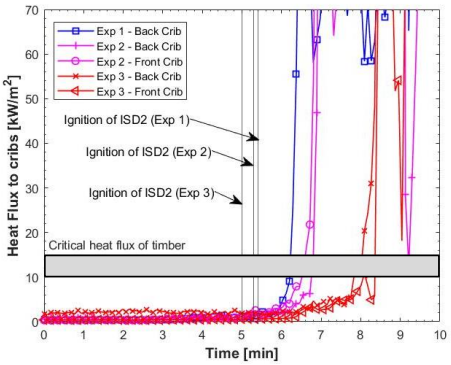

Fig. 26. Incident heat flux received by cribs (experimental results)

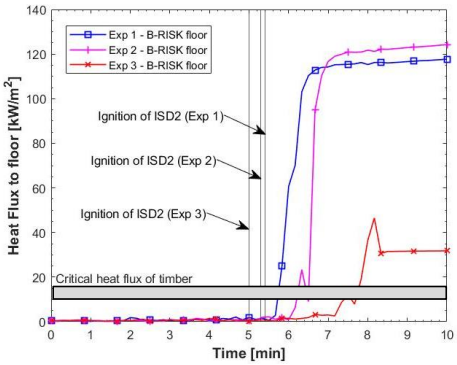

Fig. 27. Incident heat flux received by cribs (numerical results)

Fig. 26 shows that the heat flux to the cribs before ignition is negligible (i.e., significantly lower than the critical heat flux of the crib timber pieces, which is around 10-15 kW/m^2 [27,28]~~[28,29]~~). However, it is clear that as soon as the fire spread rate across the surface of cardboard lining starts to accelerate, the energy release, and subsequently the heat fluxes emitted to crib level, is significant (i.e., > 100 kW/m^2) and is more than enough to induce flashover. By considering the time from ignition of ISD2 to the onset of flashover of ISD2 (both looking at Fig. 26 and Fig. 27), it is clear that the more ventilation present at ceiling level, the longer the time to the onset to flashover, i.e. since more openings allow the hot gases to escape from the enclosure quicker.

5. PARAMETRIC STUDY

Comparing the numerical results above to the experimental results, it is clear that B-RISK does capture the overall behavior of the ISDs studied in this work, at most measurement locations (e.g., the upper layer temperature and velocities of hot gases leaving the enclosure), well. There are however certain measurements where the experimental and numerical results do not compare well, e.g. the mass flow of air entering the enclosure. The authors are, however, uncertain why there are such discrepancies and are uncertain whether the problem is numerical or experimental, although it is possibility related to the permeable nature of the dwellings and the interactions with wind. However, with the exception of the inflow velocities, B-RISK can be used for a parametric investigation with a fair level of confidence. In this section, the following ventilation parameters are further investigated: a) the window aspect ratio (keeping the area of the opening the same and the window soffit at 1.85 m), b) the window opening size (keeping the aspect ratios the same and the window soffit at 1.85 m) and c) the sill height of the window (keeping both the opening size and aspect ratio the same). The effects of leakages and ventilation conditions on IS fire spread are not well understood and how these conditions should be incorporate in statistical fire spread models [9,10] for IS dwellings are unclear. Hence, if simple tools, like B-RISK, can be used to determine these effects, it would be beneficial for the further development of these statistical models.

For all the simulations that follow, the geometry of the ISD of Exp 1 is used, with the same inputs as described in Section 3 above. However, in this case a simplified HRR curve was assigned to each crib, as depicted in Fig. 28, as opposed to the measured HRR. The heat release rate of the crib was determined using Equations 2-4 above and it was found that the crib is porosity-controlled.

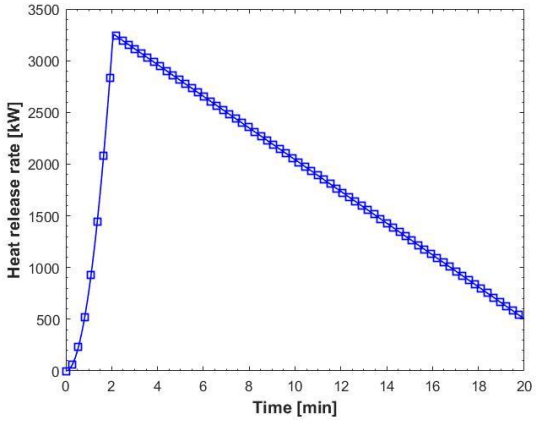

Fig. 28. Heat release rate input used per crib in B-RISK

5.1. Window aspect ratio

In this section, the effect of the window aspect ratio on the maximum upper layer temperature, gas flow velocities and the time to flashover are investigated, while keeping the window area the same. Table 4 summarizes the numerical inputs and outputs of this parametric study. In all cases, the window soffit height was kept at 1.85 m as per experiments.

Table 4: Summary of the numerical inputs and outputs for the window aspect ratio parametric study.

Scenario	Window aspect ratio (H/W)	Window area (m^2)	Maximum upper layer temperature (°C)	Maximum door velocity (m/s)	Time to flashover (s)
Baseline (BL)	0.71	0.51	947	5.79	66
Scenario 2 (S2)	1.25	0.51	942	5.8	65
Scenario 3 (S3)	1.96	0.51	936	5.82	65
Scenario 4 (S4)	2.82	0.51	934	5.88	65
Scenario 5 (S5)	3.84	0.51	935	5.97	65

The results listed in Table 4 clearly shows that the window aspect ratio has a negligible effect on the maximum upper layer temperature, gas flow velocities and the time to flashover. The parameter most affected is the gas flow velocities. It appears that as the aspect ratio increases, the maximum gas flow velocity at the door increase, implying that the horizontal flame length will increase, which increases the probability of flame impingement onto the adjacent dwelling.

5.2. Window opening size

In this section, the effect of the window opening size on the maximum upper layer temperature, gas flow velocities and the time to flashover is investigated, while keeping the window aspect ratio the same. Table 5 summarizes the numerical inputs and outputs of this parametric study. In all cases, the window soffit height was kept at 1.85 m as per experiments.

Table 5: Summary of the numerical inputs and outputs for the window area size parametric study.

Scenario	Window area (m^2)	Ventilation factor ($m^{1.5}$)	Maximum upper layer temperature (°C)	Maximum door velocity (m/s)	Time to flashover (s)
Baseline (BL)	0.51	0.4	947	5.79	66
Scenario 2 (S2)	0.9	0.81	966	5.67	68
Scenario 3 (S3)	1.41	1.41	979	5.66	71

Scenario 4 (S4)	2.03	2.22	985	5.77	74
Scenario 5 (S5)	2.76	3.27	928	5.73	79

The results depicted in Table 5 indicate that as the opening size (and as a result the opening factor) increases, the maximum upper layer gas temperature increases. This is true for Scenario 1 (BL scenario) to Scenario 4, however once the ventilation controlled HRR surpasses the maximum HRR of the fuel (6.4MW) the maximum gas temperature starts to decrease as the opening size (and as a result the opening factor) increases. One can easily determine the critical ventilation factor at which the fully developed fire will no longer be ventilation controlled using Equation 1, where $\dot{m}$ is set equal to the maximum HRR of the fuel divided by the heat of combustion of the fuel:

$$\frac{6400}{17000} = 0.12A_o\sqrt{H_o} \quad (6)$$

this then gives a ventilation factor ($A_o\sqrt{H_o}$) of 3.14 $m^{1.5}$ (this point is referred to as the critical ventilation limit for the rest of this section). Hence, for Scenario 4 we can clearly see that the fire is still ventilation controlled during the fully developed fire stage (i.e., 2.22 < 3.14 $m^{1.5}$) and thus the gas temperature increased, but Scenario 5 is now fuel controlled during the fully developed fire stage (i.e., 3.27 > 3.14 $m^{1.5}$) and thus the gas temperature started to decrease. This implies that adding or removing openings or changing their size will only have the benefit of decreasing the gas temperatures if it results in a real ventilation factor sufficiently above or below that of the critical ventilation limit. Assuming the critical ventilation limit as a baseline, it is noteworthy that a small increase in ventilation area from this critical value will result in a greater reduction in gas temperature than an equal decrease in area. However, this must be treated as a trade-off with the fact that lower opening areas will result in lower configuration factors between the openings and receiving dwellings. Thus, if an ISD has a high fuel load density [3,29][~~3,16~~] or contains naturally fast-burning fuels, one must be careful to ensure that a change to the openings does not increase the fire spread risk by moving the ventilation factor closer to the critical value. However, in a scenario where the ISD has a low fuel load or slow burning materials, the critical ventilation limit will be a lower value and so there is a much higher probability that adding openings will consistently increase the ventilation factor above the critical value, thus decreasing temperatures. Additionally, if the receiving (target) dwelling has more openings it increases the probability of the dwelling being ignited, because there are more spaces for flames to impinge on combustibles.

The B-RISK parametric results in Table 5, further highlights that as the ventilation factor increases, the time to flashover increases. This is well known within the fire community and can be described in terms of the following equation [30][~~30~~]:

$$\dot{Q}_{FO} = 610\left(h_k A_T A_o\sqrt{H_o}\right)^{1/2} \quad (7)$$

where $\dot{Q}_{FO}$ is the minimum HRR needed for flashover to occur, h_k is the effective heat transfer coefficient (h_k for thermally thin boundaries, such as informal settlement boundaries, has been investigated in depth by Beshir et al. [31]) and A_T is the total enclosing area of the compartment. Hence, from Equation 7, it is clear that as the ventilation factor increases, the minimum HRR needed for flashover increases, implying that the time to reach that HRR will increase.

Formatted: Font color: Black

5.3. Window soffit height

In this section, the effect of the window soffit height on the maximum upper layer temperature, gas flow velocities and the time to flashover is investigated, while keeping the window aspect ratio and area the same. Table 6 summarizes the numerical inputs and outputs of this parametric study.

Table 6: Summary of the numerical inputs and outputs for the window soffit height parametric study.

Scenario	Window soffit height (m^2)	Maximum upper layer temperature (°C)	Maximum door velocity (m/s)	Time to flashover (s)
Baseline (BL)	1.85	947	5.79	66
Scenario 2 (S2)	1.65	938	5.81	65
Scenario 3 (S3)	1.45	927	5.84	64
Scenario 4 (S4)	1.25	918	5.95	64
Scenario 5 (S5)	1.05	918	6.10	64

Comparing Tables 4-6 it is clear that the window soffit height has the largest effect on both the maximum gas temperature reached and the maximum door gas flow velocities reached. Considering Fig. 29, it becomes clear that as the soffit height increases, the height of the neutral plane height increases. This then leads to a decrease in the gas flow velocities at the door (meaning shorter horizontal flames emerging from the door), which allows for less hot gases to leave the enclosure (i.e., less heat loss by convection) allowing for higher gas temperatures (meaning higher radiation being emitted).

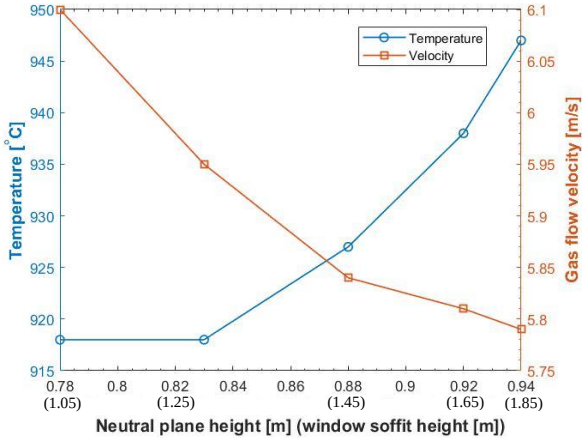

Fig. 29. The effect of the window soffit height on a) the neutral plane height, b) the gas temperature and c) the gas flow velocities at the door

6. CONCLUSION

This paper investigated the effects of leakages and ventilation conditions on the fire dynamics in informal settlements, with a key interest on the fire spread behavior. This work will be beneficial for the development of ~~computational~~ statistical fire spread models that can approximately predict fire spread through informal settlements. Ignition and time-temperature, or time-heat flux, sub-models of individual homes can be defined in more detail based on the results obtained (i.e., since this work showed that simple two-zone model software can be used to generate these sub-models for statistical fire spread models, as opposed to complex computational fluid dynamics software)~~.~~

In this work, 3 full-scale informal settlement experiments were conducted. Each experiment consisted of two dwellings. The differences between the three experiments were kept to a minimum, with only one leakage or ventilation condition being changed from experiment to experiment. B-RISK (a two-zone fire model software) was used to simulate the three experiments conducted in this work. The B-RISK results showed relatively good correlation to the experimental results, thus the software was further utilized by conducting a parametric study on the following ventilation parameters: a) the window aspect ratio (keeping the area of the opening the same), b) the opening size (keeping the aspect ratios the same) and c) the sill height of the window (keeping both the opening size and aspect ratio the same).

- The data showed that having leakages (i.e., open flutes), ISD2 experiences less heat build-up which means that once the cardboard lining ignites, the spread rate across the surface is reduced as a result of a reduction in the preheating of the cardboard. Additionally, leakages cause the peak HRR inside the dwelling to slightly increase, as a result of the increase in the ventilation factor. Leakages did, however, not significantly influence the maximum flame lengths ejecting from the door or the heat fluxes emitted from the openings. This is beneficial for future computational modelling as it is not easy to account for the presence of the commonly found small openings in people's homes.
- It was observed that adding a roof vent significantly reduced the flame lengths from the door opening and also reduced the heat fluxes emitted from the door opening, reducing spread in the direction of side openings. However, the data further indicated that a roof vent significantly increased the peak HRR, by around 40%, since it raises the neutral plane significantly, allowing more oxygen to enter the dwelling and hence changing the burning regime from ventilation-controlled to fuel-controlled. The plume emitted radiation in all directions with calculated fluxes in the order of 20 kW/m^2 at 2 m, meaning that fire can spread radially (possibly igniting combustible roof linings such as plastic sheets) and not only in the directions defined by side openings.
- The parametric study showed that changing the opening aspect ratios had virtually no effect of the enclosure fire dynamics. Assuming ISDs have a high fuel load density, the parametric studied showed that more openings increase the probability of a dwelling igniting its neighboring dwelling, and also increases the probability of the dwelling being ignited, but it does however delay the time to flashover once ignited.

7. ACKNOWLEDGEMENTS

The authors would like to gratefully acknowledge Breede Valley Fire Department and two undergraduate students, Monique Scheepers and Kyle Stebbing, from Stellenbosch University for their contribution and assistance towards helping the authors

successfully complete the experiments. This work is financially supported by IRIS-Fire GCRF project from the UK (Engineering and Physical Sciences Research Council Grant no.: EP/P029582/1), the Lloyd's Register Foundation under the "Fire Engineering Education for Africa" project (Grant GA 100093).

8. REFERENCES

[1] City of Cape Town, Increase in residential fires and related fatalities are cause for concern, (2019).

[2] UN-Habitat, Slum Almanac 2015/2016: Tackling Improvement in the Lives of Slum Dwellers, Nairobi, 2016.

[3] R. Walls, G. Olivier, R. Eksteen, Informal settlement fires in South Africa: Fire engineering overview and full-scale tests on "shacks," Fire Safety Journal. 91 (2017) 997–1006. https://doi.org/10.1016/j.firesaf.2017.03.061.

[4] A. Cicione, M. Beshir, R.S. Walls, D. Rush, Full-Scale Informal Settlement Dwelling Fire Experiments and Development of Numerical Models, Fire Technology Journal. (2019). https://doi.org/10.1007/s10694-019-00894-w.

[5] Y. Wang, L. Gibson, M. Beshir, D. Rush, Determination of Critical Separation Distance Between Dwellings in Informal Settlements Fire, Fire Technology. (2021). https://doi.org/10.1007/s10694-020-01075-w.

[6] A. Cicione, R.S. Walls, C. Kahanji, Experimental study of fire spread between multiple full scale informal settlement dwellings, Fire Safety Journal. 105 (2019) 19–27. https://doi.org/10.1016/j.firesaf.2019.02.001.

[7] M. Beshir, K. Omar, F.R. Centeno, S. Stevens, L. Gibson, D. Rush, Experimental and numerical study for the effect of horizontal openings on the external plume and potential fire spread in informal settlements, Applied Sciences (Switzerland). 11 (2021). https://doi.org/10.3390/app11052380.

[8] M. Beshir, A. Cicione, Y. Wang, S. Welch, D. Rush, Re-visiting NIST Reduced / Full-Scale Enclosures (R / FSE) Experiments (2007-2008), in: Interflam Proceedings, 2019: pp. 2095–2107.

[9] A. Cicione, C. Wade, M. Spearpoint, L. Gibson, R.S. Walls, D. Rush, A preliminary investigation to develop a semi-probabilistic model of informal settlement fire spread using B-RISK, Fire Safety Journal. 120 (2021).

[10] A. Cicione, L. Gibson, C. Wade, M. Spearpoint, R. Walls, D. Rush, Towards the development of a probabilistic approach to informal settlement fire spread using ignition modelling and spatial metrics, Fire. 3 (2020) 1–26. https://doi.org/10.3390/fire3040067.

[11] Y. Wang, M. Beshir, A. Cicione, R. Hadden, M. Krajcovic, D. Rush, A full-scale experimental study on single dwelling burning behavior of informal settlement, Fire Safety Journal. (2020) 103076. https://doi.org/10.1016/j.firesaf.2020.103076.

[12] A. Cicione, R. Walls, Z. Sander, N. Flores Quiroz, V. Narayanan, S. Stevens, D. Rush, The effect of separation distance between informal dwellings on fire spread rates based on experimental data and analytical equations, Fire Technology. (2020).

[13] A. Cicione, M. Beshir, R.S. Walls, D. Rush, Full-Scale Informal Settlement Dwelling Fire Experiments and Development of Numerical Models, Springer US, 2019. https://doi.org/10.1007/s10694-019-00894-w.

[14] N. de Koker, R.S. Walls, A. Cicione, Z.R. Sander, S. Löffel, J.J. Claasen, S.J. Fourie, L. Croukamp, D. Rush, 20 Dwelling Large-Scale Experiment of Fire Spread in Informal Settlements, Fire Technology. 56 (2020). https://doi.org/10.1007/s10694-019-00945-2.

[15] A. Cicione, R.S. Walls, C. Kahanji, Experimental study of fire spread between multiple full scale informal settlement dwellings, Fire Safety Journal. 105 (2019) 19–27. https://doi.org/10.1016/j.firesaf.2019.02.001.

[16] M. Beshir, Y. Wang, L. Gibson, S. Welch, D. Rush, A Computational Study on the Effect of Horizontal Openings on Fire Dynamics within Informal Dwellings, Proceedings of the Ninth International Seminar on Fire and Explosion Hazards (ISFEH9. (2019) 512–523. https://doi.org/10.18720/spbpu/2/k19-122.

[17] CEN, Eurocode 1: Actions on structures -Part 1: General actions - Actions on structures exposed to fire, CEN, 2002.

[18] M.A. Delichatsios, Fire Growth Rates in Wood Cribs, Combustion and Flame. 27 (1976) 267.

[19] V. Babrauskas, Heat release rates, in: M.J. Hurley et. al (Ed.), SFPE Handbook of Fire Protection Engineering, 5th ed., Springer, 2016: p. 829. https://doi.org/10.1007/978-1-4939-2565-0.

[20] C. Wade, G. Baker, K. Frank, R. Harrison, M. Spearpoint, BRANZ Study report SR364 B-RISK 2016 user guide and technical manual, 2016.

[21] A. Tewarson, Generation of Heat and Chemical Compounds in Fires, in: P.J. DiNenno (Ed.), SFPE Handbook of Fire Protection Engineering, 3rd ed., 2016: pp. 277–324. https://doi.org/10.1007/978-1-4939-2565-0_9.

[22] B.J. McCaffrey, J.G. Quintiere, M.F. Harkleroad, Estimating room temperatures and the likelihood of flashover using fire test data correlations, Fire Technology. 17 (1981) 98–119. https://doi.org/10.1007/BF02479583.

[23] M.A. Delichatsios, Fire Growth Rates in Wood Cribs, Combustion and Flame. 27 (1976) 267.

[24] B. Karlsson, J.G. Quintiere, Enclosure fire dynamics, CRC Press, London, New York, Washington D.C., 2000. https://doi.org/10.1016/S0379-7112(01)00031-5.

[25] A.I. Bartlett, R.M. Hadden, L.A. Bisby, A Review of Factors Affecting the Burning Behaviour of Wood for Application to Tall Timber Construction, Fire Technology. 55 (2019) 1–49. https://doi.org/10.1007/s10694-018-0787-y.

[26] W. Jaskolkowski, P. Ogrodnik, A. Lukaszek-Chmielewska, The study of time to ignition of woods external heat flux by piloted ignition and autoignition, Annals of Warsaw University of Life Sciences - SGGW. Forestry and Wood Technology. 86 (2014) 133–137.

[27] Y. Wang, C. Bertrand, M. Beshir, C. Kahanji, R. Walls, D. Rush, Developing an experimental database of burning characteristics of combustible informal settlement dwelling materials, Fire Safety Journal. (2019). https://doi.org/https://doi.org/10.1016/j.firesaf.2019.102938.

[28] Y. Wang, D. Rush, Cone calorimeter tests of combustible materials found in informal settlements, [dataset], (2019).

[29] A. Cicione, R.S. Walls, C. Kahanji, Experimental study of fire spread between multiple full scale informal settlement dwellings, Fire Safety Journal. (2019). https://doi.org/10.1016/j.firesaf.2019.02.001.

[30] D. Drysdale, An introduction to fire dynamics, 3rd ed., Wiley, Chichester, 2011.

[31] M. Beshir, M. Mohamed, S. Welch, D. Rush, Modelling the Effects of Boundary Walls on the Fire Dynamics of Informal Settlement Dwellings, Fire Technology. (2021). https://doi.org/10.1007/s10694-020-01086-7.